Distributed Power Control Algorithms for WCDMA Cellular Systems

Gaurav Pradeep Mandhare

A Thesis

in

The Department

of

Electrical and Computer Engineering

Presented in Partial Fulfillment of the Requirements

for the Degree of Master of Applied Science

Concordia University

Montreal, Quebec, Canada

June 2006

Your file Votre référence
ISBN: 978-0-494-20752-9
Our file Notre référence
ISBN: 978-0-494-20752-9

Abstract

Distributed Power Control Algorithms for WCDMA Cellular Systems

Gaurav Pradeep Mandhare

In this thesis, we propose two power control algorithms, one signal-to-interference (SIR) based and the other bit-error-rate (BER) based. The proposed algorithms are of first order and have been devised for use as distributed power control algorithms for the uplink channel in wideband code division multiple access (WCDMA). The main feature of the proposed algorithms is that they use a nonlinear power update function which helps in improving the convergence speed of these algorithms. We study the convergence of the proposed algorithms and show that they always converge to a fixed point. We examine the algorithms in time varying multipath Rayleigh fading environments with a wide range of terminal mobilities. We demonstrate that the proposed algorithms converge faster than existing power control algorithms, including the 3GPP standard algorithms. We also demonstrate that the proposed algorithms result in gains in the required signal-to-noise ratio (SNR) between 1.0 dB to 1.5 dB for the SIR-based algorithm and about 1.0 dB for the BER-based algorithm, all relative to the 3GPP standard power control algorithms.

Dedicated to my family.....

Acknowledgments

First of all, I would like to express my sincere appreciation to my academic supervisor Dr. Ali Ghrayeb for giving me invaluable support, constructive guidance and helpful discussion. I am grateful for his patience and kindness in answering my questions and revising my reports. Without his continuous encouragement and stimulating suggestions, I would not have succeeded.

I would also like to thank Xiang Nian Zeng and Mohamed Abou-Khousa in our research group. They generously provided me with a lot of suggestions and help in my research and thesis. I also want to thank all the people who helped me throughout my study at Concordia University.

Finally, I would like to thank my parents for their love, trust and encouragement. Without their support, it would have been impossible for me to accomplish what I have accomplished.

Contents

List of Figures

List of Tables

Chapter 1

Introduction

The third generation mobile systems (known as 3G or Universal Mobile Telecommunications System (UMTS)) are designed to accommodate multimedia communication applications. With these technologies, peer to peer communications can be enhanced using higher data rate communication. In the standardization process, Wideband Code Division Multiple Access (WCDMA) has come up as the most widely adopted third generation air interface technology. The specifications for WCDMA are defined in 3GPP (3rd Generation Partnership Project) which is the joint standardization project of the standardization bodies from Europe, Japan, Korea, USA and China.

1.1 WCDMA

Wideband CDMA standard is designed to support variable data rates upto 2 Mbps to the end user with a bandwidth utilization of around 5 MHz. The interface uses

the CDMA technology which is based on the principle of spread spectrum (SS). This means that the user information bits are multiplied by a spreading sequence and spread over a wide frequency bandwidth. All the user equipments (UEs) in the system transmit on the same frequency at the same time while using the total bandwidth by each user. Contrary to this, wireless transmission system, such as Global System for Mobile (GSM) communications, which work on the principle of time division multiplexing (TDM), share the total available bandwidth among the users.

Spread spectrum techniques are commonly divided into two types [1], which are

- Direct Sequence (DS-SS): Data is scrambled by user specific pseudo noise code at the transmitter side.
- Frequency Hopping (FH-SS): The signal is spread by changing the frequency during the transmission time of the signal. This can further be classified as Fast Frequency or Slow Frequency Hopping.

WCDMA uses the DS-SS technique for its operation. WCDMA operates in the $1920 - 1980$ MHz band for the uplink and $2110 - 2170$ MHz for the downlink. Compared with the Time Division Multiple Access (TDMA) system, it provides better network frequency planning since the same radio frequency can be used for the neighboring base stations (BSs). There are two basic modes of operation in WCDMA systems, namely, Frequency Division Duplex (FDD) and Time Division Duplex (TDD). In FDD, transmission and reception is done simultaneously on two different radio frequencies, i.e., separate 5 MHz carrier frequencies are used for uplink and downlink.

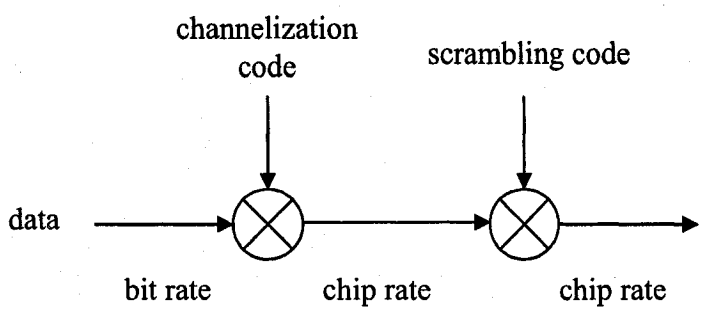

Figure 1.1: Basic WCDMA transmitter system.

In the TDD mode, the same radio frequency is used for transmission and reception. So, only one 5 MHz carrier is time shared for the two operations. Thus, TDD a mixture of TDMA and CDMA.

1.2 Spreading and Despreading

Fig. 1.1 shows the basic operation taking place in WCDMA systems at the transmitter end. The process consists of multiplying the user data information by a channelization code and a scrambling code, respectively. The channelization codes decide the spreading factor for the transmit signal depending on the bit rate requirement of the user. Thus, the bits are converted into chips form after spreading and the baseband signal is spread over wideband. The scrambling codes are then used for cell/user separation. It does not affect the chip rate. Fig. 1.2 shows a sequential procedure of the actual operation taking place in a WCDMA system. As shown, the number of chips in one bit duration decides the spreading factor. This produces the spread

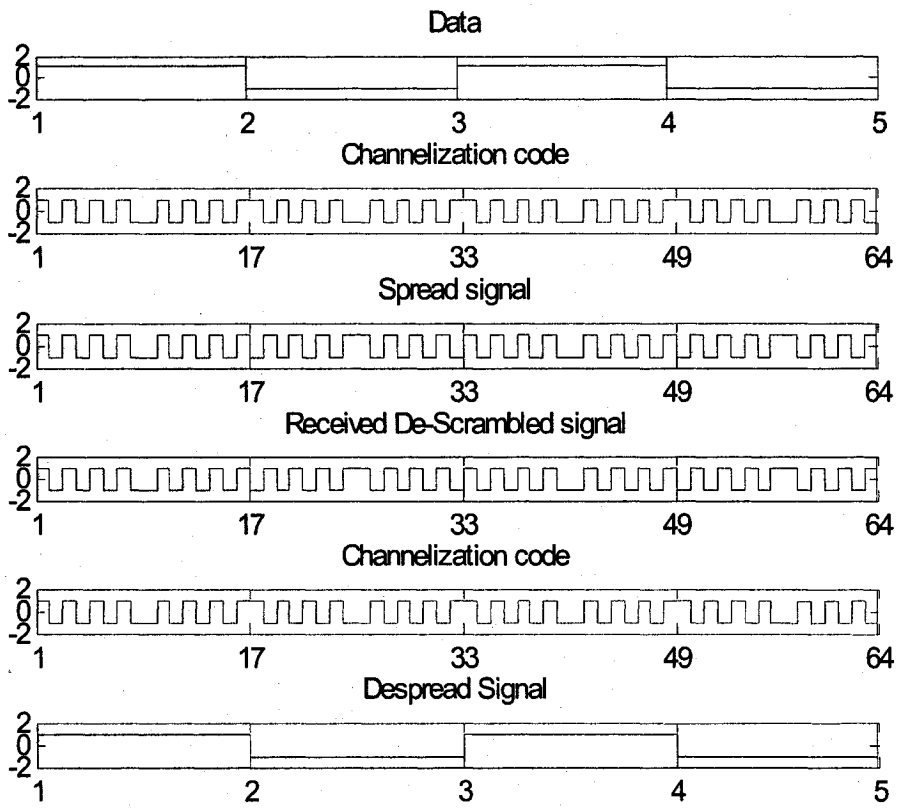

Figure 1.2: Spreading and despreading operation.

signal of bit rate equal to the chip rate. This operation increases the bandwidth of the actual signal and makes it a wideband signal as shown in Fig. 1.3.

The spread signal transmitted from the transmitter adds up with the additive noise and interference from other users. At the receiver end, the spread signal is multiplied by the same spreading (channelization) code. This time, multiplication by the spreading code gives the original user information back. Also, when the interference signal is multiplied with this spreading code, it becomes a wideband signal with power

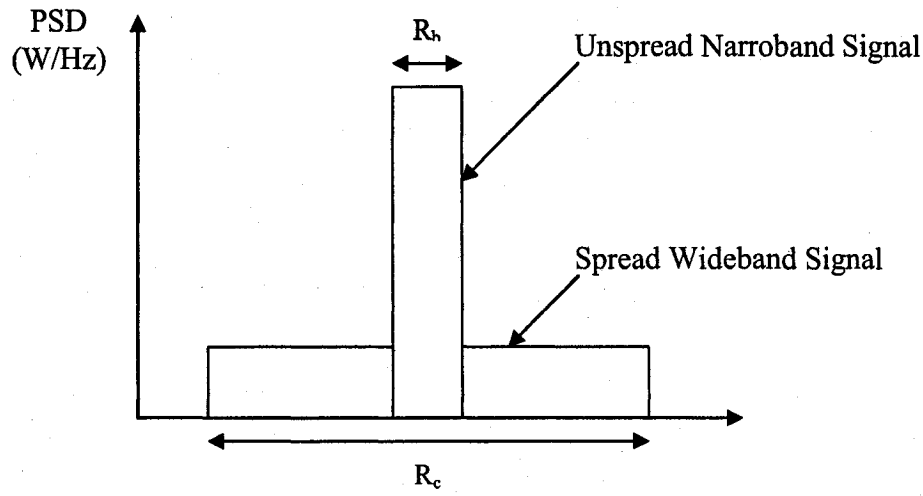

Figure 1.3: Spectrum of the spread signal.

spread all over the spectrum. In this situation, the intended signal dominates interference and can be detected easily. Using different codes for different users allows the users to use the same frequency band. Security in communication is thus maintained since only the intended user can decode the information by using the appropriate despreading code.

1.3 Physical Channel Structure

WCDMA defines two dedicated physical channels in both directions:

- Dedicated Physical Data Channel (DPDCH) to carry dedicated data generated at layer 2 and above.

- Dedicated Physical Control Channel (DPCCH) to carry layer 1 control information.

Each connection is allocated one DPCCH and zero, one or more DPDCHs. In addition, there are common physical channels defined as:

- Primary and Secondary Common Control Physical Channels (CCPCH) to carry downlink common channels.
- Synchronization Channels (SCH) for cell search.
- Physical Random Access Channel (PRACH) for the call setup from UE to BS.

1.4 I-Q Multiplexing

As we discussed previously, WCDMA consists of two dedicated physical channels, DPDCH and DPCCH. These channels can be either time multiplexed or code multiplexed. In the uplink direction, data may not be present all the time on the DPDCH channel but control information will always be there on the DPCCH channel as shown in Fig. 1.4. Therefore, time multiplexing will produce pulsed transmission at rate 1500 Hz which comes in human audible range. Thus it may cause electromagnet compatibility (EMC) problems.

To avoid EMC problems, DPDCH and DPCCH are I-Q code multiplexed (called dual channel QPSK modulation). Now since data and control information are transmitted on separate channels, no pulsating transmission occurs due to discontinuity.

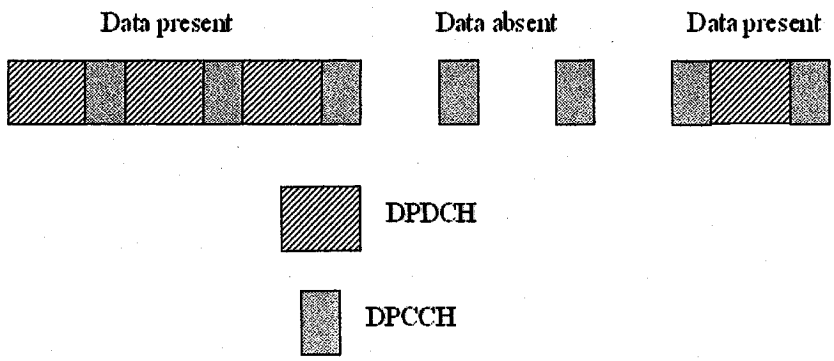

Figure 1.4: Time multiplexing of data and control channel.

The I-Q code multiplexing is shown in Fig. 1.5.

1.5 Spreading and Modulation

The spreading concept is applied to physical channels and consists of two operations. The first is the channelization operation which transforms each data symbol into a number of chips, thus increasing the bandwidth of the signal. The number of chips per data symbol is called the spreading factor (SF). This operation uses a pseudo noise like wideband code to spread the information signal. The second operation is scrambling where a scrambling code is applied on top of the spread signal. This operation does not change the bandwidth, but randomizes the signal. Spectrum spreading is the act of increasing the bandwidth of an information signal to be transmitted to a remote radio receiver. The receiver despreads the signal to recover the original information signal.

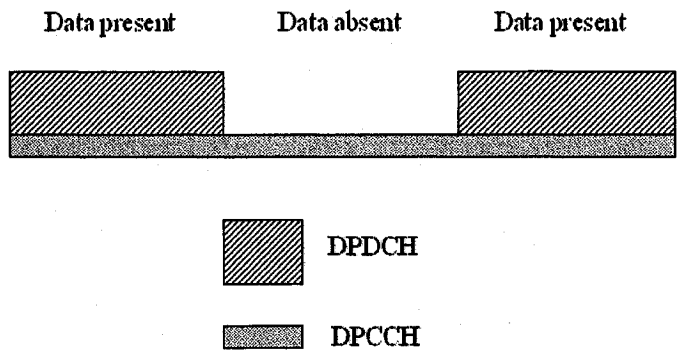

Figure 1.5: Code multiplexing of data and control channel.

In wideband CDMA systems, the two types of codes mainly used are:

1.5.1 Channelization Codes

Channelization codes serve two purposes in WCDMA system. The first is to spread the baseband signal to the chip rate (3.84 Mcps), and the second is for user identification (downlink) or the data/control channel separation (uplink). The channelization codes used, both in uplink and downlink, are Orthogonal Variable Spreading Factor (OVSF) codes [5] that preserve the orthogonality between downlink channels of different rates and spreading codes. A channelization code $C_{ch,SF,N}$ is uniquely described by two numbers: the SF in the range $[4 - 256]$ ($[4 - 512]$ in downlink) and the identification number (ID) N = [0 to SF-1]. The control channel is always spread by the code $C_{ch,256,0}$ which consists of 256 logic zeros. When only one data channel is transmitted, data channel, is spread by code $C_{SF,p}$ where $p = \frac{SF}{4}$. When more than

one data channel is transmitted, all of the data channels have a spreading factor equal to 4 [9].

The OVSF codes are generated from a single base Walsh-Hadamard matrix, given as

$$H_{2N} = \begin{bmatrix} H_N & H_N \\ H_N & -H_N \end{bmatrix}.$$

The channelization code length is in the form of 2^n, where n is greater than or equal to 2. Note that the length of the code is also equal to the spreading factor (SF= 2^n). The channelization codes in WCDMA can use different length OVSF codes to achieve variable rate transmission. The code tree structure is shown in Fig. 1.6. When an OVSF code is selected, the subtree codes will be blocked and will not be usable in the same physical channel, e.g., referring Fig. 1.6, if the code $C_4(1)$ is selected, the spreading codes in the subtree ($C_8(3)$, $C_8(4)$, ...) are all blocked.

In the channelization process, the bipolar data symbols on the I and Q branches are independently multiplied by an OVSF code, which is aligned in time with the symbol boundary. The OVSF codes are effective only when the channels are perfectly synchronized at the symbol level. The loss in crosscorrelation is compensated for by the additional scrambling operation.

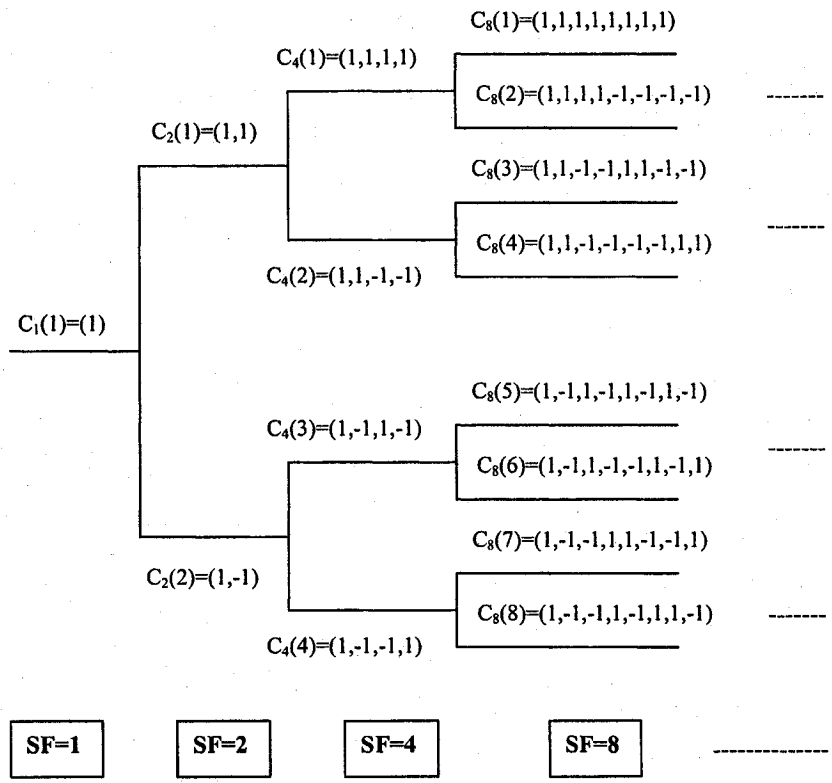

Figure 1.6: OVSF code tree structure.

1.5.2 Scrambling Codes

In addition to spreading, part of the process in the transmitter is the scrambling operation. Scrambling provides separation of users/cells. It is used on top of spreading and does not affect the transmission bandwidth. With scrambling, it would not matter if the actual spreading is done with identical code for several transmitters. With the scrambling operation, the real (I) and imaginary (Q) parts of the spread signal are further multiplied by a complex-valued scrambling code. The scrambling code sequences are constructed by combining two real-valued *m-binary sequences* into a complex sequence. Each of the two real sequences are constructed as the position-wise modulo-2 sum of 38400 chip segments of two binary m-sequences generated by means of two generator polynomials. The scrambling codes are repeated for every 10 ms radio frame.

1.6 Uplink Channel

1.6.1 Uplink Spreading and Modulation

The uplink spreading and modulation process is illustrated in Fig. 1.7. One DPCCH and up to six parallel DPDCHs can be spread and transmitted simultaneously. For the DPDCH/DPCCH spreading, the binary dedicated physical channels are first mapped to $+1$ or -1 and then spread by the channelization codes. The DPCCH is always spread using the channelization code $C_{ch,256,0}$ which consists of 256 logic zeros. When only one DPDCH is transmitted, the spreading factor may vary on a frame-by-frame

basis. If more than one DPDCH is transmitted, the spreading factor will be fixed at 4. After spreading, the signals are weighted by the gain factors β_d (for DPDCH) and β_c (for DPCCH) and then summed for I and Q branches separately. These I and Q signals are then treated as a complex-valued chip stream $(I + jQ)$ and scrambled by the scrambling code.

Any discontinuity in the uplink transmission may cause audible interference to audio equipment close to terminal. A typical example is the interference caused by the GSM transmission frame frequency (217 Hz) caused by GSM terminals. In order to avoid this effect, the DPDCH and DPCCH are I/Q multiplexed instead of time multiplexing as discussed before.

1.6.2 Uplink Scrambling

For the uplink, each UE has its own scrambling code which is assigned by higher layers. The code can be either long or short. The long scrambling codes are Gold codes which are truncated to 10 ms frame length (38400 chips with 3.84 Mcps). The long scrambling codes are used if the base station uses a Rake receiver. The short scrambling codes are 256-chips long Extended S(2) code family. If advanced multiuser detectors or interference cancellation receivers are used in the base station, short scrambling codes can be used to make the implementation of the advanced receiver structures easier. There are 2^{24} long and 2^{24} short scrambling codes. Since millions of codes are available, no uplink code planning is needed.

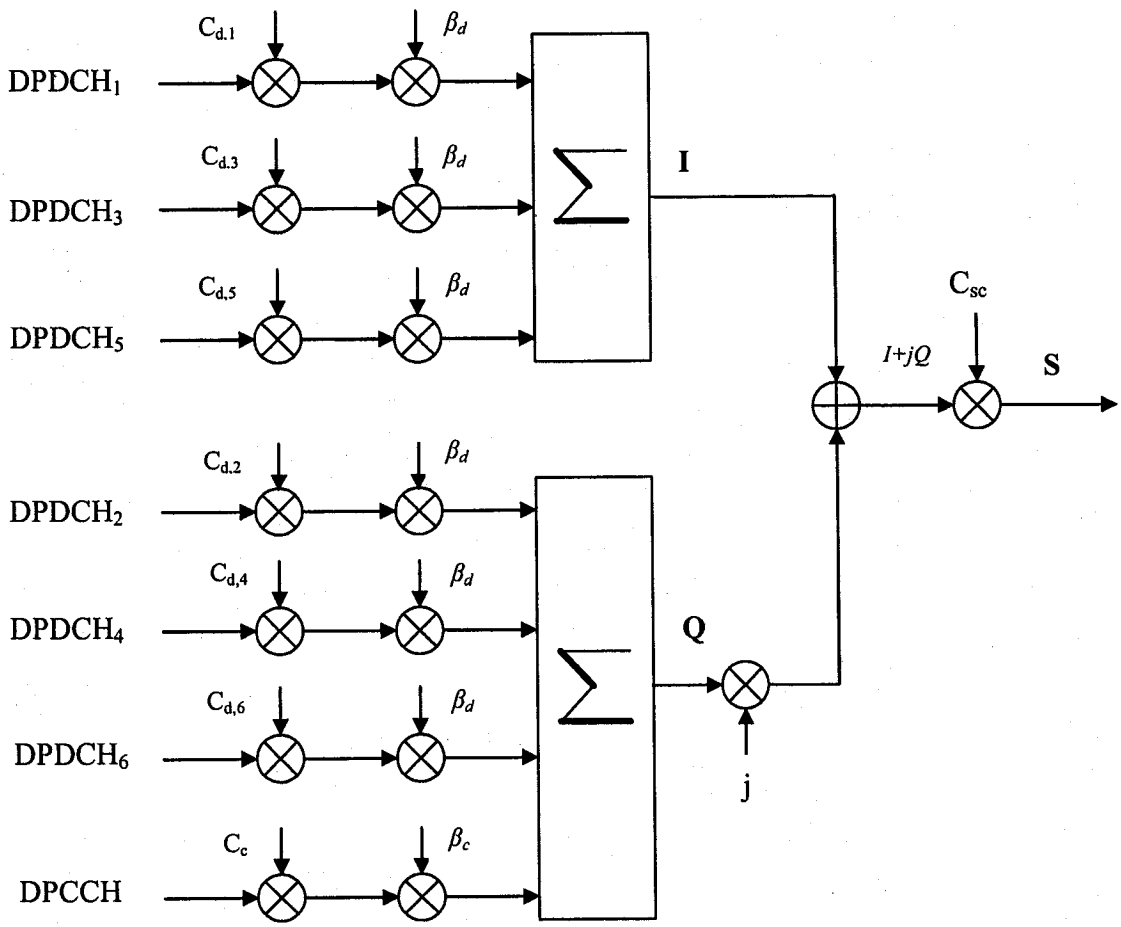

Figure 1.7: Uplink spreading and scrambling operation.

Properties of m-sequences

1. The number of 1's in a maximal-length binary sequence is more than the number of 0's by one. The number of 1's in the sequence is (N+1)/2.

2. The modulo-2 sum of an m-sequence and any phase shift of the same sequence is another phase of the same m-sequence (shift and add property).

3. If a window of width r is slid along the sequence for N shifts, each r-tuple except the all zero r-tuple will appear exactly once.

4. Define a run as a subsequence of identical symbols within the m-sequence. The length of this subsequence is the length of the run. Then, for any m-sequence, there is

   - 1 run of ones of length r.
   - 1 run of zeros of length $r-1$.
   - 1 run of ones and 1 run of zeros of length $r-2$.
   - 2 runs of ones and 2 runs of zeros of length $r-3$.
   - 4 runs of ones and 4 runs of zeros of length $r-4$.

     $\vdots$

   - 2^{r-3} runs of ones and 2^{r-3} runs of zeros of length 1.

5. The autocorrelation function can be depicted as in Fig. 1.8.

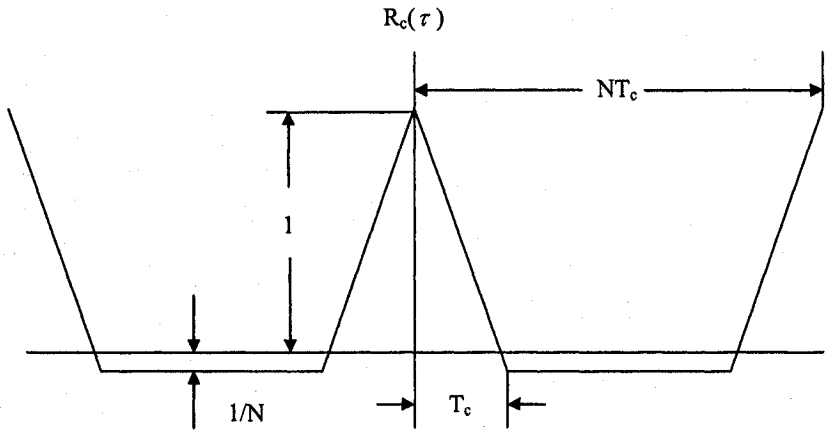

Figure 1.8: Autocorrelation of an m-sequence code.

Long Scrambling Codes

The long codes are essentially Gold codes. Large sets of Gold codes have low cross-correlation properties so that as many users as possible can use the channel with minimum mutual interference. Two m-sequence generator polynomials are used to generate the long scrambling codes. The generator polynomials are $x^{25} + x^3 + 1$ and $x^{25} + x^3 + x^2 + x + 1$. These 25-degree generator polynomials are truncated to the 10 ms frame length. The long scrambling sequences, $c_{1,n}$ and $c_{2,n}$, are constructed from a position-wise modulo-2 sum of 38400 chip segments of the two binary m-sequences.

1.6.3 Uplink Frame Structure

Fig. 1.9 shows the uplink frame structure for the dedicated physical channels. In the uplink, DPDCH and DPCCH are I/Q code multiplexed using complex scrambling codes. The DPDCH is transmitted on the I channel whereas control information

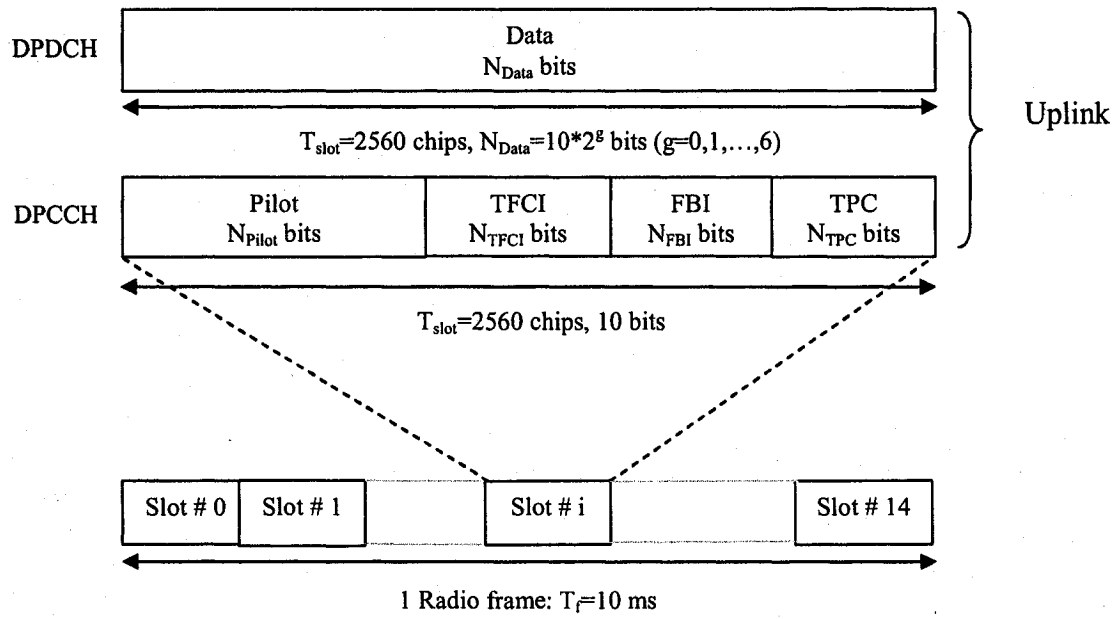

Figure 1.9: Uplink frame structure.

contained in the DPCCH is transmitted on the Q channel. The information to be transmitted is divided into different frames of length 38400 chips or 10 ms with each frame containing 15 slots and thus 15 power control periods. Each user is allocated frames of 10 ms duration, during which the user data rate is kept constant. The DPCCH consists of predefined pilot symbols (used for channel estimation and coherent detection), transmit power control (TPC) commands, feedback information (FBI) for closed-loop mode transmit diversity and site selection diversity technique (SSDT) and an optional transport format combination indicator (TFCI). There can be zero, one or several DPDCHs but only one DPCCH on each radio link.

The parameter g in Fig. 1.9 determines the number of bits in each slot. The parameter is related to the SF as SF $= \frac{256}{2^g}$. The spreading factor thus has a range of

4 to 256. The spreading factor is selected according to the data rate required.

1.7 Downlink

1.7.1 Downlink Spreading and Modulation

All downlink physical channels, except for the synchronization channel, are first serial-to-parallel mapped onto I and Q branches. The I and Q branches are then spread to the chip rate by the same channelization code $C_{ch,SF,m}$. The channelization code is the same OVSF code mentioned in Section 1.5. The spread signal is then multiplied by a complex scrambling code $S_{dl,n}$ which represents the nth downlink scrambling code for cell/sector separation. Balanced QPSK modulation is implemented with time multiplexing of data and control streams. Since the common channels in the downlink have continuous transmission, there will not be any audible interference when data and control information is time multiplexed. The data modulation is QPSK for the downlink whereas it is BPSK for uplink. The data rates on the I and Q channels are the same in the downlink whereas the data rates on the I and Q channel of the uplink may be different. Fig. 1.10 shows the spreading and modulation process for downlink.

1.7.2 Downlink Scrambling

The downlink scrambling codes are used to maintain cell or sector separation. The downlink scrambling uses long codes, the same Gold codes as in the uplink. The

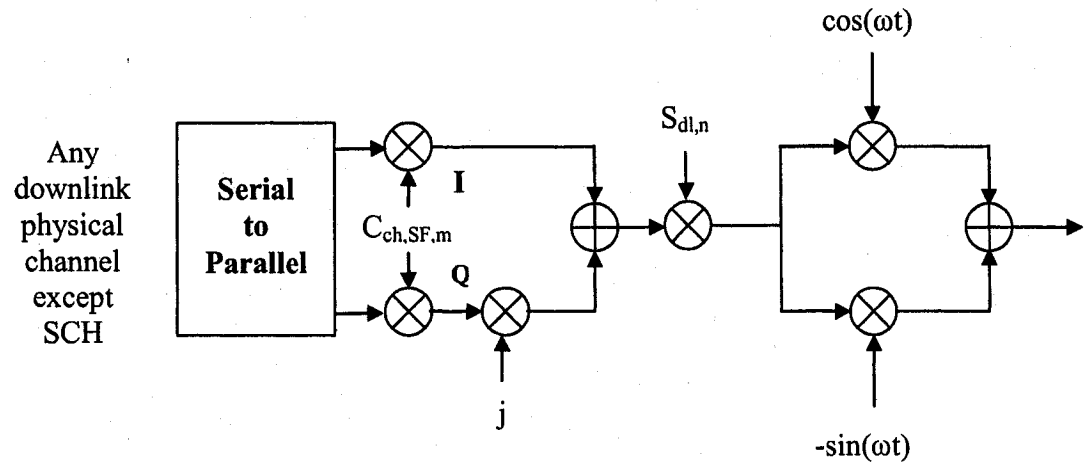

Figure 1.10: Downlink spreading and scrambling.

complex valued scrambling code is formed from a single code by simply having a delay between the I and Q branches. The code period is 10 ms and $2^{18}-1$ distinct scrambling codes can be generated. The downlink set of the (primary) scrambling codes is limited to 512 codes in order to simplify the cell search procedure by the UE.

The downlink scrambling codes are generated in the same way as the uplink scrambling codes. However, the sequence is constructed using the generator polynomials $x^{18}+x^7+1$ and $x^{18}+x^{10}+x^7+x^5+1$. Both the polynomials are primitive over GF(2). Fig. 1.11 shows the shift register structure for generating the downlink scrambling code.

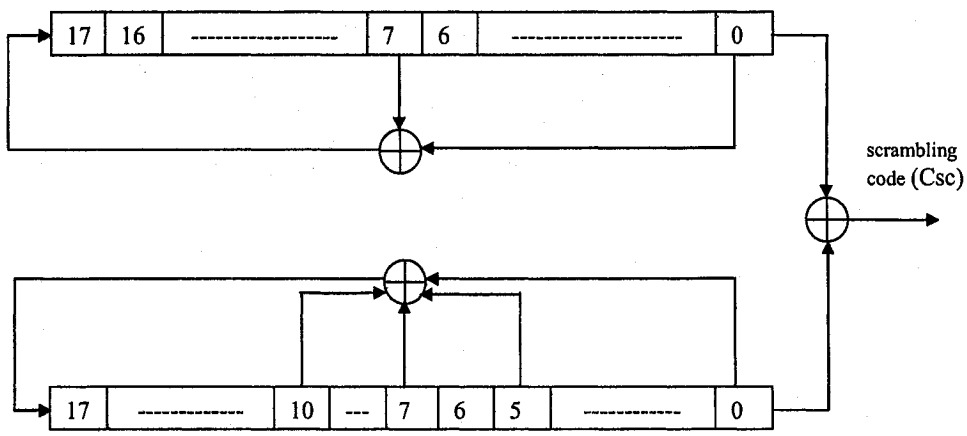

Figure 1.11: Downlink scrambling code geneartor.

1.7.3 Downlink Frame Structure

In the downlink, the dedicated physical channel (DPCH) consists of DPDCH and DPCCH time-multiplexed with complex scrambling. Therefore, the dedicated data generated at higher layers carried on DPDCH is time-multiplexed with pilot bits, TPC commands and TFCI bits (optional). Fig. 1.12 shows the exact representation of the downlink frame structure.

The parameter g is related to the spreading factor as $\mathrm{SF} = \frac{512}{2^g}$. Thus the spreading factor has a range of 4 to 512. The exact number of bits of these different uplink DPCCH fields and downlink frame are given in [7].

We summarize in Table I the discussion on the spreading and modulation applied to the WCDMA system [2] and [3].

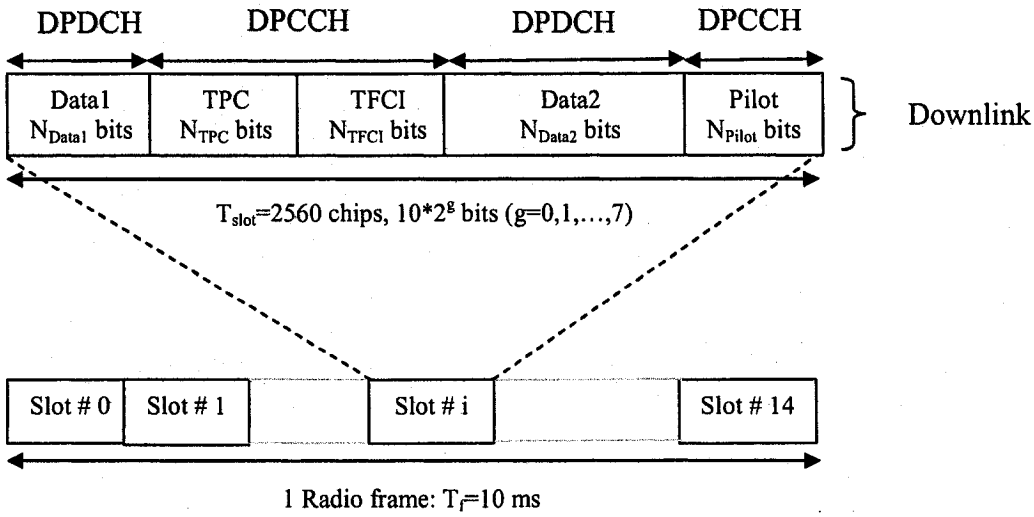

Figure 1.12: Downlink frame structure.

Table 1.1: WCDMA performance parameters.

Carrier spacing	5 MHz
Chip rate	3.84 Mcps
Frame length	10 ms (38400 chips)
Number of slots/frame	15
Number of chips/slot	2560 chips
Uplink SF	4 to 256
Downlink SF	4 to 512
Base station synchronization	Not needed
Spreading modulation	Balanced QPSK (downlink), Dual channel QPSK (uplink)
Data modulation	QPSK (downlink), BPSK (uplink)
Spreading and Scrambling (downlink)	Variable length orthogonal sequence for channel separation. Gold sequences 2^{18} for cell separation (truncated cycle 10 ms)
Spreading and Scrambling (uplink)	Variable length orthogonal sequence for channel separation. Gold sequences 2^{41} for user separation (truncated cycle 10 ms)

1.8 Radio Resource Management

In wireless systems, it is very important to manage the available system resources. Resource management is especially important when the number of users and the demand for bandwidth increases. In such cases, effective allocation and utilization of resources will improve the performance and increase the capacity. The Radio Resource Management (RRM) algorithms include Admission Control (AC), Load Control (LC), Packet Scheduler (PS), Handover Control (HC) and Power Control (PC) [3].

Different types of traffic may have different information bit rates and different quality-of service (QoS) requirements. One controllable radio resource, highly related to the network capacity, is the transmit power. The capacity of the WCDMA system is limited by the total interference, called multiple-access interference (MAI). MAI is therefore a dominant factor in the system capacity and quality of communications, and must be suppressed or reduced if a high capacity cellular mobile system with a satisfactory performance is to be implemented. One effective way of reducing MAI is to control each mobile transmit power to be at the minimum level to achieve a certain performance level. Transmit power control and assignment is therefore a critical issue for WCDMA systems.

1.9 Power Control

One of the important resource management issues in WCDMA is power control. Since all the users transmit on the same carrier frequency, increase in the number of

users creates more interference. In this case, effective resource management is really important to maintain the system performance. If the transmitted signals of all the mobile stations are at the same power level, a strong signal from a near-in mobile will mask the weak signal from a far-end mobile station. The stronger signals cause unnecessary interference on the reverse links (uplink) of other mobile stations unless they are controlled. This gives rise to the so-called near-far effect by which the system capacity is limited.

1.9.1 Need for Power Control

- Mitigate the near-far problems by providing the minimum power required for each connection,
- Reduce the interference in the network,
- Increase the capacity of the system, and
- Reduce battery power consumption.

1.9.2 Classification of Power Control Techniques

Power control algorithms can be mainly categorized as either centralized or distributed. In centralized power control, a central device collects the data and controls the power of all the devices. Distributed power control (DPC) is performed at each cell and does not need a large database. However, the unavailability of the global information takes longer time for the DPC algorithms to reach to the near-optimum

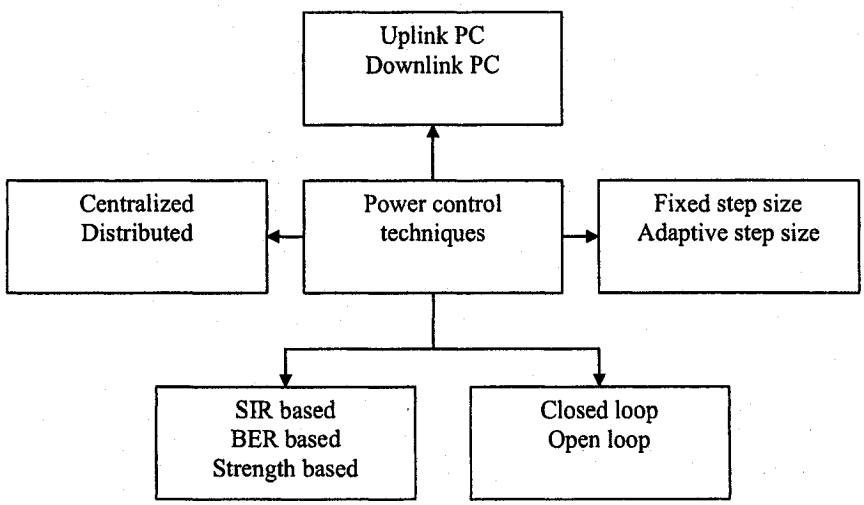

Figure 1.13: Classification of power control techniques [4].

power level as compared to the centralized algorithms. Hence, the convergence speed and condition of the DPC algorithms become important issues.

Power control in WCDMA is mainly comprised of three mechanisms, which are:

1. Open Loop Power Control

   The open loop power control adjusts the initial access power of a mobile station and compensates for abrupt changes in propagation conditions. Here, the power is updated based on the estimates of the propagation loss which is obtained by measuring the received signal strength at the receiver.

2. Closed Loop Power Control

   Since the fast fading channel is not fully correlated on uplink and downlink,

closed loop power control is used. The signal strength is measured at the receiver end. According to the estimated level, a power up or down command is transmitted to the mobile. The closed loop power control performance is deteriorated by feedback delays, imperfect power estimates and feedback channel errors. The power control command react cycle is 1500 times per second (1.5 KHz) for each mobile station which is faster than any fading mechanism.

3. Outer Loop Power Control

   The outer loop power control is done at the Radio Network Controller (RNC). In closed loop power control, estimated signal strength is compared with a target value. The comparison parameter can be either signal-to-interference ratio (SIR) or bit error rate (BER) of the received signal. The target value is different for different propagation conditions. The outer loop power control adjusts the target value in order to obtain a certain BER or related quantity such as frame error rate (FER). Outer loop power control update frequency is $10 - 100$ Hz.

Recent research concentrated more on the distributed schemes than on the centralized ones because centralized power control requires large-scale data management and induces network vulnerability.

Uplink Power Control

Uplink power control is important to combat fading and the near-far problem. In the closed-loop uplink power control, the base station needs to set SIR to a given SIR_{tgt} to maintain a certain QoS for all mobile stations. After comparing the received SIR from the mobile station with the reference value, the base station sends either a power up or power down command. The base station sends a power control command to a mobile station at a rate of 1500 bps so that the mobile station maintains reliable QoS with minimum transmitted power. The power control command is updated every 0.667 ms. This is to compensate for the near-far problem.

Downlink Power Control

The downlink power control adjusts the power transmitted by the base station to the mobile station. Thus, the mobile transmits the power control command to the base station. This is to provide more power to the user at the cell edge as compared to other users.

Fig. 1.13 shows a general classification of the power control algorithms. The power control can be strength based, SIR based or BER based. BER is a better quality measure since SIR is time variant. The algorithms can also be discriminated on the basis of fixed step size and adaptive step size. Since the measurement of the average received power is in practice very difficult, power control based on SIR is more preferable [10]. In addition, SIR, not the received power, determines the bit error probability of the user. By utilizing SIR, both the near-far problem and control

of MAI are addressed. Thus SIR-based fast closed loop distributed power control algorithm is widely used for its simplicity.

1.10 Thesis Outline

The rest of the thesis is outlined as follows.

In Chapter 2, we study few existing SIR-based and BER-based algorithms. In this chapter, we reproduce the results of some of the algorithms under consideration.

In Chapter 3, we present the least mean square (LMS) algorithm. We use a modified form of the LMS algorithm and propose a SIR-based power control algorithm. This non-linear power update algorithm is mathematically analyzed to justify its convergence. Simulation results support the mathematical analysis. The mobility of the UE is also taken into account during the simulations.

In Chapter 4, after a brief discussion of the BER as a decision criterion, we propose an efficient BER-based power control algorithm. We mathematically analyze the algorithm and guarantee the convergence of the algorithm. Finally, the simulation results support the mathematical analysis and demonstrate better performance of the proposed algorithm.

In Chapter 5, we make conclusions with respect to the simulation results for the SIR-based and BER-based algorithms and suggest directions for future research.

1.11 Thesis Contributions

The main contributions of the thesis can be summarized as follows:

- We propose a novel SIR-based power control algorithm and compare the same with the 3GPP Algorithm-1 [8] and exponential function algorithm [13]. We use a modified form of the LMS algorithm using an exponential function to improve the system performance.
- We analyze the convergence of the proposed algorithm and prove its guaranteed convergence.
- We show a better convergence speed and lower average required SNR value by the proposed algorithm compared to the other two algorithms over a frequency selective Rayleigh fading channel. It is shown that a gain of 1 dB to 1.5 dB is is achieved in the required SNR value.
- Considering the simplicity of measurement, we propose a BER-based power control algorithm. The BER-based proposed algorithm is mathematically analyzed to assure its convergence.
- The performance of the BER-based algorithm is compared with the 3GPP Algorithm-1 and a previously proposed BER-based algorithm [29]. We demonstrate that the algorithm shows quick convergence properties. A gain of around 0.5 dB to 1 dB is achieved in the average required SNR value. The algorithm is also shown to perform better in high mobility environments.

Chapter 2

Ordinary Transmit Power Control

2.1 Introduction

In this chapter, we discuss a few of the previously proposed power control algorithms. The discussion begins with the transmitter and receiver structure of the WCDMA system. The discussion includes already proposed SIR-based and BER-based algorithms. We discuss the advantages and disadvantages of these proposed algorithms. We reproduce the results for the standard 3GPP proposed algorithm [8] and an exponential update function algorithm [13]. Finally, we make some remarks on the results obtained.

2.2 System Model

Fig. 2.1 shows the transmitter and receiver model simulated for testing the power control algorithms investigated in this chapter. Here, the uplink of the frequency

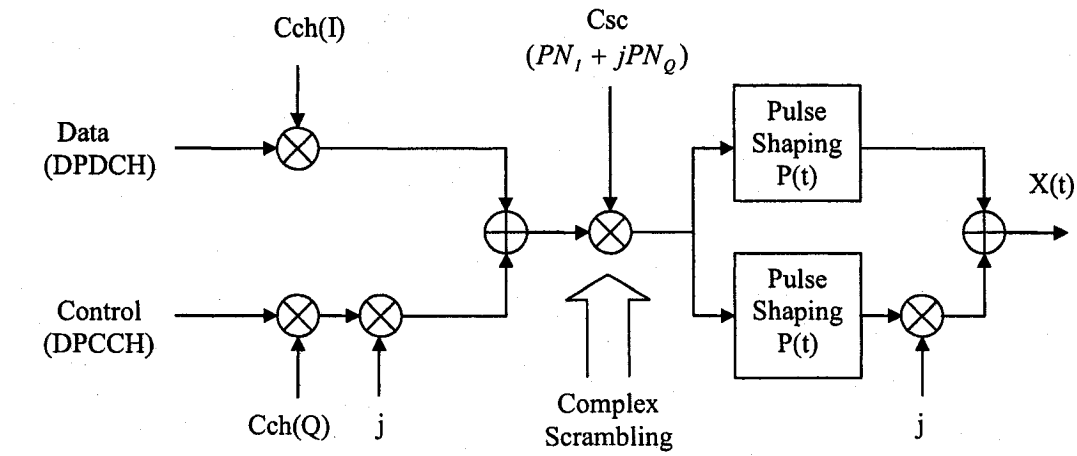

(a)

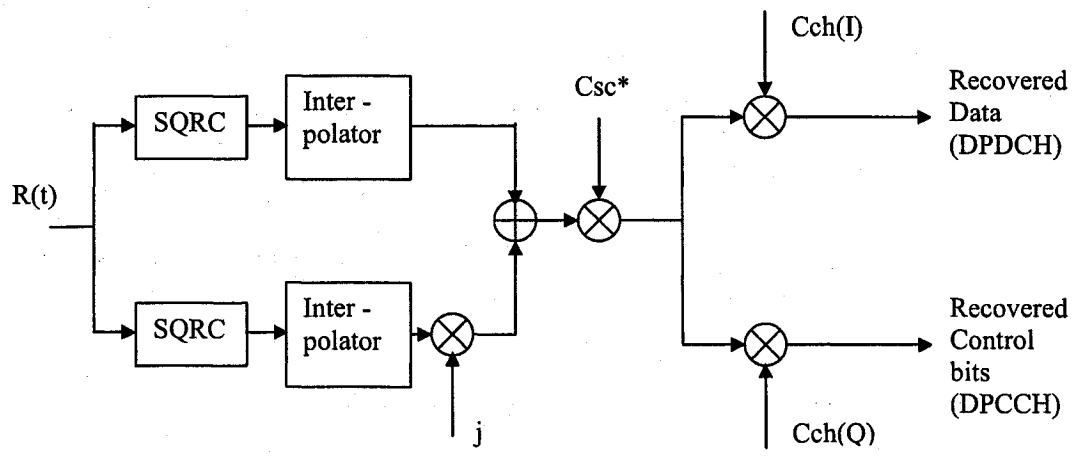

(b)

Figure 2.1: (a) Transmitter model for uplink direction of Wideband CDMA system; (b) Receiver model for uplink direction of Wideband CDMA system (single path).

division duplex (FDD) WCDMA 3G system is considered for explanation. In a FDD-CDMA system, a physical channel is defined by its code and frequency. The spreading modulation used in the uplink is dual channel QPSK. Spreading modulation consists of two different operations. As shown in Fig. 2.1(a), the bipolar data and control symbols on the I and Q branches are independently multiplied by different channelization codes. In the uplink case, we prefer to use a spreading factor of 64 for the data symbols. Control bits are always spread using a spreading factor of 256. The second operation is the scrambling where a complex valued scrambling code is applied to spread signal. The complex scrambling code is a unique signature of the mobile station in the uplink direction. The users can be separated only by despreading their signals with the appropriate code. A square-root raised-cosine filter with roll-off factor 0.22 is used at the transmitter for pulse shaping. The receiver at the base station has a filter matched to the pulse shaping filter at the transmitter.

The system considered here is the same as that of the standard WCDMA. We consider a multipath RAKE receiver at the BS end. But only one out of l branches is shown in Fig. 2.1(b). The RAKE receiver takes advantage of the multipath propagation and combines several received versions of the original signal into a stronger signal. Each multipath component is called a 'finger'. To be able to combine several fingers, the RAKE receiver needs to know the relative delay for each finger. The RAKE receiver combines the multipath components with a separation in time of more than one chip period (T_c). Thus, the received signals separated by more than $T_c = 260$ ns (approximately 78 meters path length difference [3]) can be combined. Here we

assume perfect phase estimation so that we can cancel out the phase in each branch.

2.3 Existing SIR-Based and BER-Based Power Control Algorithms

SIR-based power control algorithms are more popular as compared to signal strength-based algorithms [6], [10] because the measurement of the average received power is difficult to accomplish in real-life applications. In addition, SIR, not the received power, determines the bit error probability of the user. Utilizing SIR also addresses both the near-far problem and control of MAI. 3GPP proposed two standard fixed step algorithms [8]. Such algorithms are attractive because they are easier to implement and need only a single bit for power control command transmission. But slower convergence speed has always been an issue for these algorithms. (The convergence speed of any power control algorithm is the most important criterion by which one determines the practical applicability of the algorithm.) The operation of the inner loop power control adjusts the power of the DPCCH channel and DPDCH channels by the same amount provided there are no changes in the gain amount [8]. The uplink power control adjusts the transmit power of the UE in order to keep the received uplink SIR close to the given SIR_{tgt}. The base station (BS) should estimate the SIR value of the received uplink DPCH channel and transmit the command to the UE accordingly.

At the UE, the command is decoded according to the power control algorithm

used and the step size, Δ_{DPCH}, is decided as:

$$\Delta_{\text{DPCH}} = \Delta_{TPC} \cdot TPC_{\text{command}}, \tag{2.1}$$

where Δ_{TPC} is the unsigned step size and TPC_{command} represents the "power up" or "power down" action. The step size is equal to 1 or 2 dB in WCDMA systems. Step size smaller than 1 dB can be emulated using more than one power control command per decision, e.g., to achieve a step size of 0.5 dB, power update decision is taken after every 2 slots. A fixed step size algorithm is simple to implement and need only 1 bit for the power control command. But the convergence is slow. On the other hand, adaptive step size algorithms have faster convergence, but require larger bandwidth as compared to fixed step size algorithms since the step size need to be transmitted in a quantized form.

SIR-based power control is aimed at controlling the SIR at the receiver end to be nearly equal to a constant value. From a practical point of view, SIR-based power control is preferable since it is the SIR, not the received power alone, that determines the QoS [6]. SIR-based control is especially important when a user is near the cell boundary facing fading and AWGN intercell interference. In this case, controlling only the received power to be stable does not give a stable SIR and QoS. Thus, SIR needs to be stabilized and not the signal power itself.

Until now, many SIR based power control algorithms have been proposed. 3GPP proposed two standard algorithms [8]. These algorithms use a fixed step size power

update. Let SIR_{est} denotes the estimated value of the SIR at the BS and SIR_{tgt} denotes the target value of the SIR to be achieved. The first algorithm is referred to as Algorithm 1, and is described as follows:

If $\text{SIR}_{\text{est}} > \text{SIR}_{\text{tgt}}$, then the TPC_{command} to transmit is "0", requesting a transmit power decrease.

If $\text{SIR}_{\text{est}} < \text{SIR}_{\text{tgt}}$, then the TPC_{command} to transmit is "1", requesting a transmit power increase.

When TPC_{command} is "0", the step size is multiplied by "-1" to decrease the transmit power. TPC_{command} equal to "1" implies multiplying step size by "1" to increase the transmit power.

3GPP proposed another algorithm termed Algorithm 2 [8] which is a slight variant of Algorithm 1. Here, the UE shall process the received TPC commands on a 5-slot cycle, where the sets of 5 slots shall be aligned to the frame boundaries and there shall be no overlap between each set of 5 slots. The value of TPC command shall be derived as follows:

- For the first 4 slots of a set, $TPC_{\text{command}} = 0$.
- For the fifth slot of a set, the UE uses hard decisions on each of the 5 received TPC commands as follows:

  - If all 5 hard decisions within the set are 1, then $TPC_{\text{command}} = 1$ in 5th slot.
  - If all 5 hard decisions within the set are 0, then $TPC_{\text{command}} = -1$ in 5th slot.
  - Otherwise $TPC_{\text{command}} = 0$ in the 5th slot.

Since the step size is fixed, these algorithms are slower in terms of convergence. A solution to this problem is to use an adaptive step size algorithm. Ling Lv *et al.* [13], [14] proposed an adaptive step size algorithm based on an exponential power update function. Here, the power update step size is decided according to the error value and thus provides a better performance. The algorithm performs better than the 3GPP standard fixed step algorithm in terms of convergence speed. The algorithm is stated as

$$P_i^{(0)} = P$$

$$P_i^{(n+1)} = e^{k(\mathrm{SIR_{tgt}} - \mathrm{SIR}_i^{(n)})} \cdot P_i^{(n)}, \tag{2.2}$$

where k is a positive parameter which can be optimized to achieve faster convergence, $\mathrm{SIR_{tgt}}$ is the desired value of the SIR, $\mathrm{SIR}_i^{(n)}$ is the received value of the SIR at the nth iteration, $P_i^{(n)}$ is the transmit power level of the ith user during the nth iteration and P is some minimum initial transmit power level.

This algorithm gives a better performance than that of the 3GPP based conventional distributed power control algorithm for fixed mobile condition, i.e. steady state channel. But the authors assume the UEs to be stationary in their simulations, which does not show the complete robustness of the algorithm. Another approach to closed loop power control is to implement a self tuning controller with real time update of the controller parameters as mentioned in [15], [16]. The two options will be to implement the minimum variance (MV) or generalized minimum variance (GMV)

controller. GMV gives better performance than MV controller. MV is the simplest approach in self tuning control. Grandhi *et al.* [17] chose constrained power control approach and the proposed power update function is given as

$$P_i^{(k+1)} = \frac{\mathrm{SIR}_{\mathrm{tgt}}}{\mathrm{SIR}_i^{(k)}} P_i^{(k)}, \qquad k = 0, 1, \ldots K. \tag{2.3}$$

where K is the number of users. Since in a real communication system, physical limits constraint the transmit powers to be less than some maximum value $P_i^{\max}$ such as

$$0 \leqslant P_i \leqslant P_i^{\max}, \qquad i = 1, 2, \ldots, n. \tag{2.4}$$

Thus, the algorithm in (2.3) can be modified accordingly [17] to obtain

$$P_i^{(k+1)} = \min \left\{ P_i^{\max}, \frac{\mathrm{SIR}_{\mathrm{tgt}}^i}{\mathrm{SIR}_i^{(k)}} P_i^{(k)} \right\}, \qquad i = 1, 2, \ldots, n. \tag{2.5}$$

This algorithm is called as Distributed Constrained Power Control (DCPC) algorithm [18] with $P_i^{\max}$ as the constraint parameter. To improve the speed of convergence, a second order constrained power control algorithm (CSOPC) [18] can be implemented. DCPC can be used together with CSOPC to take advantage of both algorithms in terms of convergence speed. But considering loop delays and fix power

control bits, it is not easy to achieve the theoretical performance.

Subramaniam *et al.* [19] proposed a pilot power based distributed power control scheme combined with a BS assignment. The proposed scheme adjusts the transmit power of the UE and equalizes the load at the BSs in high traffic conditions. The BS estimates the total reverse link received power and transmits its forward link pilot power in inverse proportion with the total received power. The UE selects the BS with the strongest power level and transmits power that is inversely proportional to the received pilot power level. This helps to adjust the transmit power of the UE and to reduce the traffic load at the crowded BS and transfer some traffic to the lightly loaded BS.

Power control using estimation of the carrier to interference ratio (CIR) information is proposed in [20] by using the received ON-OFF commands from the feedback channel. The transmit power of the UE is adjusted using the estimated CIR with the distributed constrained power control algorithm. Here the error between the target and the received values of the CIR is estimated and is minimized iteratively. But it takes more time to converge to a target value as compared to the fixed step algorithm. Also the algorithm performs well only for slow fading. A dynamic step size power control algorithm is mentioned in [21]. The number of transmit power control (TPC) bits depends upon the number of thresholds assumed. As the number of thresholds increases, the complexity of the algorithm increases. Nasreddine *et al.* [22] proposed an adaptive power control algorithm for downlink. The novelty of the algorithm is the incorporation of the stabilization zone concept above the SIR_{tgt} for limiting the

oscillations.

In the algorithms discussed above, we can observe that the speed of convergence and outage probability are being important comparison parameters. It is also important to consider the average value of the SNR required at the receiver end. By considering this parameter, we can compare the power level at the transmitter end.

Although SIR has been a popular decision criterion [10], [11], SIR-based algorithms can face positive feedback [12], which happens when the power increase for one user increases the interference level for other users. Also, handling the positive feedbacks and their consequences are complicated because the system includes multiple BSs and the interference at each BS has an independent short-term variation [11]. SIR is time-varying and thus the average SIR will not be equal to its equivalent average BER value. This makes the BER a better quality measure. To this end, Kumar *et al.* [29] proposed a distributed power control algorithm based on BER measurement. The authors performed a mathematical analysis of the algorithm and proved that the algorithm satisfies the necessary conditions for convergence. But the documentation lacks simulation results. Buehrer *et al.* [30] also analyzed the algorithm mentioned in [29] with a different approach and proved that the power control algorithm converges to somewhat an optimum point. It was also shown that the algorithm can be used in successive interference cancellation, which is one of the efficient techniques used in multiuser detection.

2.4 Simulation Results

In our simulations, we use the system model depicted in Fig. 2.1. We reproduce the results of few of the previously proposed power control algorithms. For the SIR-based power control algorithm, we simulate the following two algorithms: 1) the 3GPP Algorithm 1 (3GPP PCA1) [8]; and 2) the exponential update function algorithm [13]. For the BER-based power control algorithm, we reproduce the results of the BER-based algorithm proposed in [29]. During the simulations, we assume 5 different users ready to transmit data and the data is received at the base station through 4 different transmission paths at relative delays of 0, 4, 8 and 12 chips. The transmitter and the receiver structure in the uplink direction considered is as shown in Fig. 2.1(a) and (b), respectively. The UEs are assumed to be mobile with a velocity of 10 km/h for all the simulation results. A carrier frequency of 1940 MHz is assumed for calculating the Doppler frequency. The Doppler frequency is normalized to 1500 Hz, i.e., to the power control frequency. The fading channel is assumed to be changing per frame. The power delay profile is assumed to be uniform. The noise is modelled as additive white gaussian noise (AWGN). Call dropping and admission control is not considered in our simulation.

2.4.1 SIR-Based Algorithm

The target SIR is fixed to 4 dB. A user data rate of 60 kbps, i.e., a spreading factor of 64 is considered for every simulation. The SIR at the receiver end is measured on

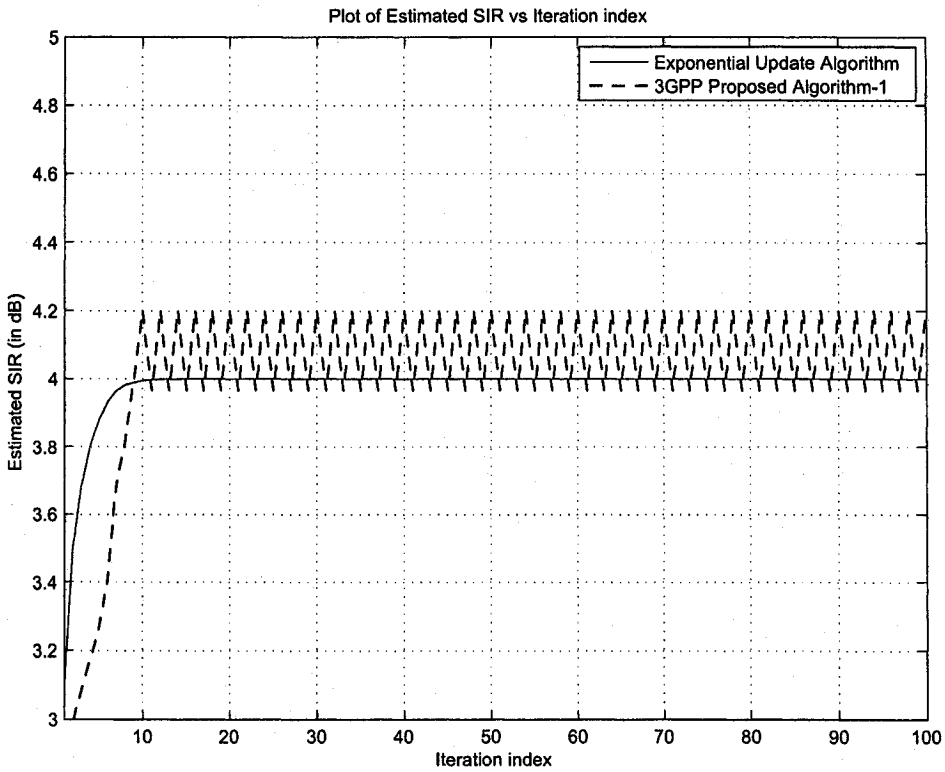

Figure 2.2: Comparison graph for 3GPP and exponential update algorithm.

the DPDCH instead of DPCCH as proposed in [25]. We also chose the frame format and the number of bits detail from [7]. In the downlink direction, slot format number 14 [7] is used ($N_{Data1} = 56, N_{Data2} = 232, N_{TPC} = 8, N_{Pilot} = 16$).

Fig. 2.2 considers the UEs to be immobile, i.e., the channel is assumed to be constant during simulations. Five users with four paths are considered. It can be easily observed that the 3GPP algorithm has poor convergence rate as compared to the exponential update function algorithm. It can also be seen that the 3GPP algorithm keeps on oscillating about the target value, whereas the exponential function algorithm is more stable.

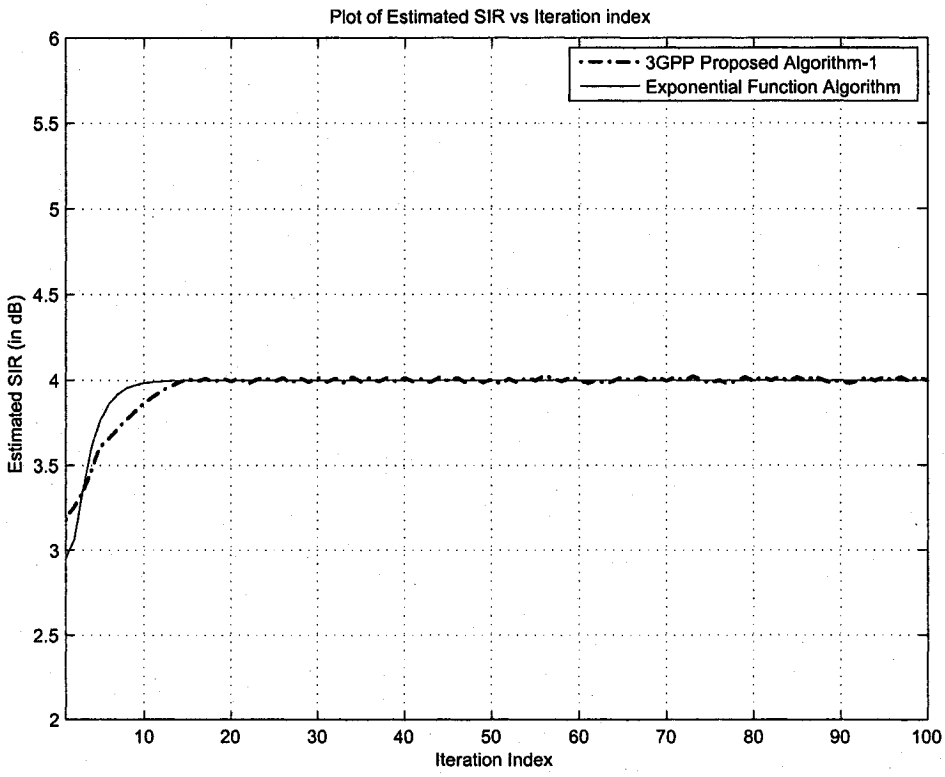

Figure 2.3: Comparison graph for 3GPP algorithm and exponential update algorithm (mobile users).

Fig. 2.3 shows the comparison between the 3GPP algorithm and the exponential function algorithm. While performing this simulation, the UEs are considered to be mobile while the channel is varying on every frame basis. Five users with two paths are considered. Since the channel is varying, moving averaging with a filter length of 20 is considered for smoothing the output. This figure clearly indicates that the exponential function algorithm has faster convergence as compared to fixed step 3GPP algorithm.

2.4.2 BER-Based Algorithm

The pilot bits on the DPCCH channel are known bits and thus can be used at the receiver end to calculate the bit error rate. Five pilot bits per slot have been chosen in the simulations. Note that, in a frame, every slot contains different sequences of zeros and ones and the frame content repeats. A spreading factor of 64 in the uplink direction has been used throughout the simulations.

Fig. 2.4 demonstrates a comparison plot of the 3GPP PCA1 and the BER-based algorithm. The figure is plotted with measured BER against the iteration index. The BER_{tgt} is set to 10^{-2}. It can be observed that the 3GPP PCA1 converges at a slower rate as compared to the BER-based algorithm and thus takes more time to stabilize.

In Fig. 2.5, we see a comparison between the 3GPP PCA1 and the BER-based algorithm when the BER_{tgt} is changed to 2×10^{-3}. In this plot, we can observe that an increase in the target BER increases the time for convergence of the 3GPP PCA1 algorithm. Comparatively, there is a very little increase in the time for convergence of the BER-based algorithm.

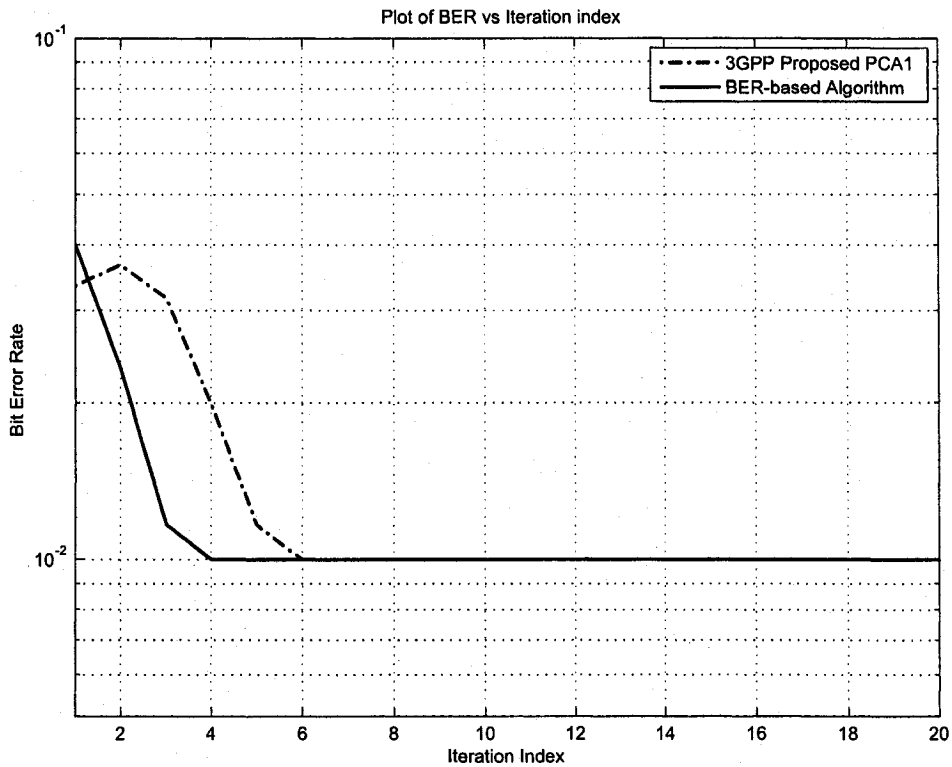

Figure 2.4: Plot of BER vs Iteration index for different algorithms with $\mathrm{BER}_{\mathrm{tgt}}$ equals 10^{-2}.

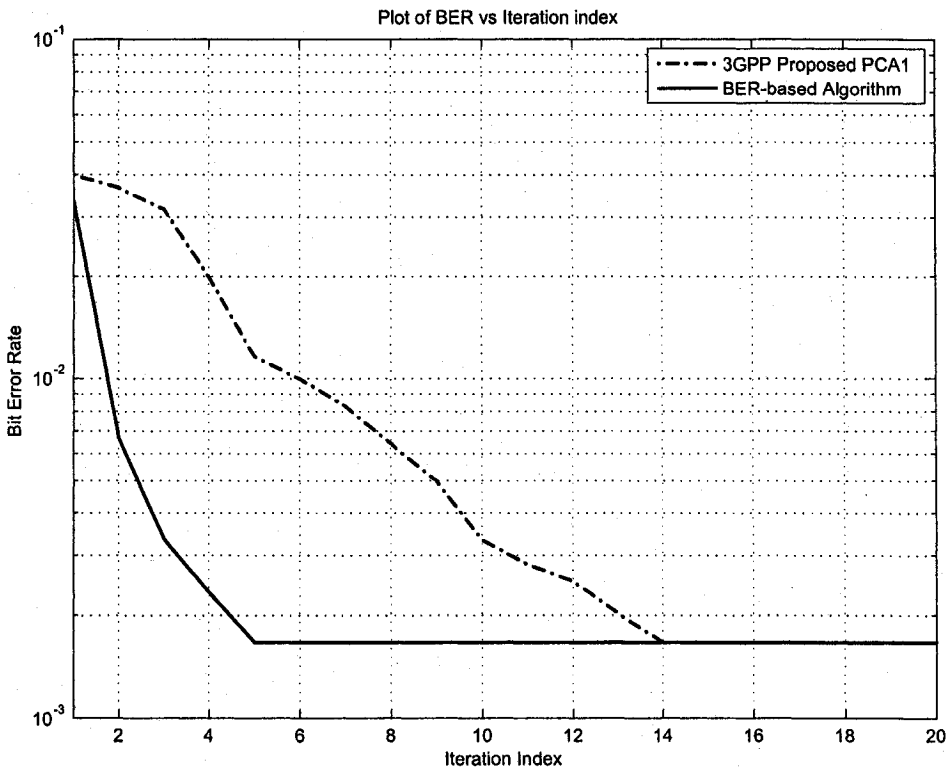

Figure 2.5: Plot of BER vs iteration index for different algorithms with $\mathrm{BER}_{\mathrm{tgt}}$ equals 2×10^{-3}.

Chapter 3

Proposed SIR-Based Power Control Algorithm

3.1 Introduction

In this chapter, we propose a novel power control algorithm. The proposed algorithm is a *SIR-based first order distributed* power control algorithm. This means that the algorithm utilizes only the recent power value and does not have to store a huge database centrally. We incorporate a modified version of the LMS algorithm to achieve a better performance than the previously proposed algorithms under consideration. We know that the LMS algorithm is widely used as a recursive update algorithm. Thus, it is useful to consider some basic properties of the LMS algorithm.

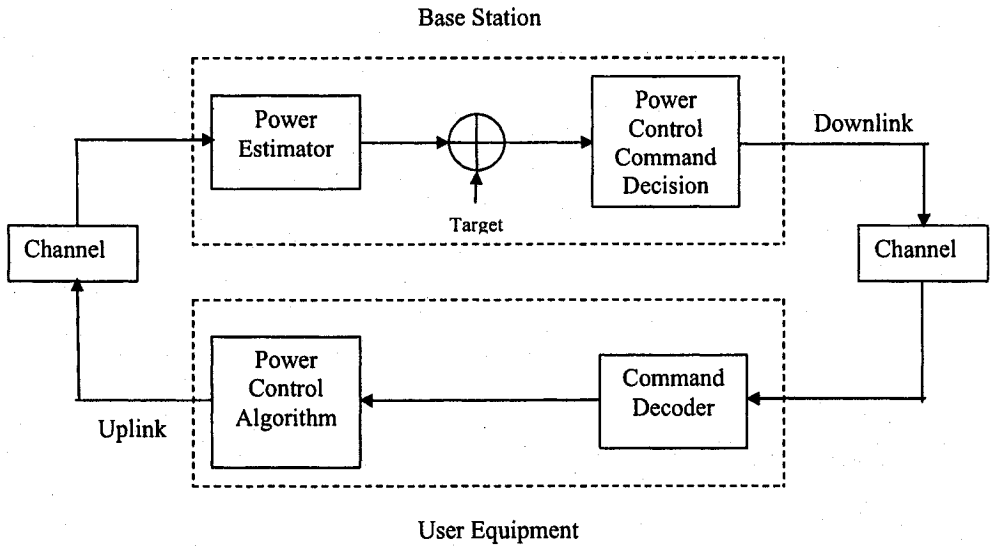

Figure 3.1: Closed-loop TPC model.

3.2 System Model

Fig. 3.1 shows the actual system model considered for the simulation purpose. It shows the block diagram of the closed-loop power control structure for uplink WCDMA. It consists of a user equipment transmitter, a base station receiver, a forward link (downlink) and a reverse link (uplink). In a conventional SIR-based power control system, the BS receives a signal from the UE. It then makes an estimate of the SIR value. This estimated value is then compared with the target SIR and accordingly, a power control command decision is taken. The command directs the UE to either increase or decrease its transmit power. Subsequently, the UE transmits the adjusted power through the reverse link.

3.3 The LMS Algorithm

The LMS algorithm is used for adaptive filtering. The algorithm uses a gradient-based method of steepest decent. The LMS algorithm iteratively updates the weight vector in the direction of the negative of the gradient vector which eventually leads to the *minimum mean square error* between its output and that of an unknown system. Using the LMS algorithm, the coefficients w_n of the predictor can be dynamically adjusted as

$$w_{n+1} = w_n + \mu x_n \xi(n), \tag{3.1}$$

where μ is an adaptation constant, x_n is the input signal and $\xi(n)$ is the prediction error.

The LMS algorithm has the advantage of simplicity in implementation and stable performance against different signal conditions. It has been used to update the weights of the power predictor dynamically in a transmit power control scheme proposed for Satellite Universal Mobile Telecommunication System (S-UMTS) [27], [28].

3.4 SIR-Based Proposed Algorithm

In Chapter 2, we discussed few proposed power control algorithms. Some of these algorithms such as the fixed step algorithm and the exponential update algorithm are easy to implement. But the fixed step algorithm has poor convergence speed.

Referring to [13], it can be seen that the exponential update algorithm does not consider the mobility of the user. The algorithm considers the users to be stationary with constant fading channel. The algorithms which follow controller approach for power update are complex in terms of implementation. We also need to consider the average SNR requirement of the system when any power control algorithm is used. Thus while proposing a new algorithm our aim is to improve the system performance in terms of convergence speed and average value of the required SNR.

As we know, the LMS criterion is an adaptive stochastic process used to adjust the weights of an adaptive filter recursively to match its output with the unknown system. The adaptive nature of the algorithm makes it capable of tracking time varying parameters. Since power is time varying in nature, we incorporate a modified form of the LMS algorithm by using an exponential function into the LMS algorithm as opposed to only an exponential function as suggested in [13]. Using such a power update function helps to improve the convergence speed of the proposed algorithm.

Let us assume that there are U users sharing the system resources simultaneously. We denote the power transmitted by the ith user as P_i where $1 \leq i \leq U$. Let Δ_1^i be the difference between the target SIR and the estimated SIR for the ith user, ($\text{SIR}_{\text{est}}^i$). In what follows, we outline the proposed SIR-based power control algorithm.

1. Transmit data from the mobile stations with predefined power level.

2. Receive the multipath transmitted data at the base station using Rake receiver.

3. Despread the actual data using corresponding spreading sequence.

4. Estimate the value of SIR from the received data.

5. If $\Delta_1^i > 0$,

$$P_i^{(n+1)} = P_i^{(n)} \cdot e^{\Delta_1^i} \cdot \mu \cdot \mathrm{SIR}_{\mathrm{est}}^i. \tag{3.2}$$

6) Else, if $\Delta_1^i < 0$,

$$P_i^{(n+1)} = \frac{P_i^{(n)} \cdot e^{\Delta_1^i}}{\mu \cdot \mathrm{SIR}_{\mathrm{est}}^i}, \tag{3.3}$$

where μ is the adaptation parameter of which we need to find the optimum value, i is the user index and n is the iteration index. When $\Delta_1^i = 0$, which is very unlikely, there will be no power update.

7) Transmit data from the mobile station with the updated value of the power level.

The use of previous or even future predicted information to assist in determining the power control command output shows an improvement in the system performance [23], [24]. Thus, using a moving averaging technique over few of the previous values to make a decision of the power control command will improve the performance of the algorithm. The SIR estimation technique used is proposed in [25]. Instead of estimating the SIR using received pilot symbols on the DPCCH channel, the SIR is estimated using received data symbols as proposed in [25] and [26] which gives

a better performance because of the large number of data bits used in making the decision.

3.5 Why Exponential Function

The idea behind using a non-linear update function came from the fact that adaptive step power control algorithms with non-linear update functions have faster convergence as compared to the algorithms with linear power update functions. Since the exponential function has good convergence properties, it will definitely improve the performance of the algorithm. We know that, for any error value, the fixed step size algorithm increases the power by some fixed amount. Thus, even if the error value is higher, the step size being fixed, it will take more number of iterations to reach to the target value. In contrast, since the exponential power update function in our algorithm is adaptive to the error value, the power update steps generated depend upon the error value. Larger is the error value, larger will be the power update step size, which makes the algorithm converge faster.

Fig. 3.2 shows an example of speed of convergence of linear and exponential functions. The exponential function $y = e^x$ is compared with two linear functions, $y = x$ and $y = 2x$. It can be seen from the figure that the exponential function takes larger steps to achieve the target and thus converges faster.

Fig. 3.3 shows an example of the speed of convergence of the exponential functions and the LMS algorithm. The exponential function $y = e^{kx}$ is compared with the LMS

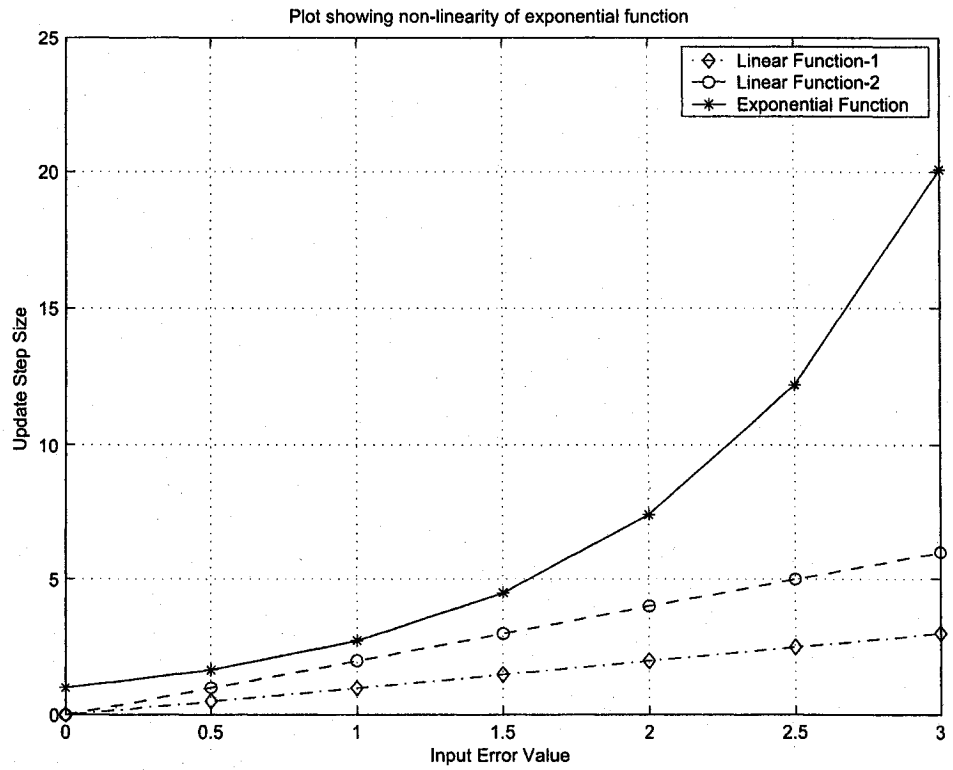

Figure 3.2: Plot of update step size against the error value for different functions.

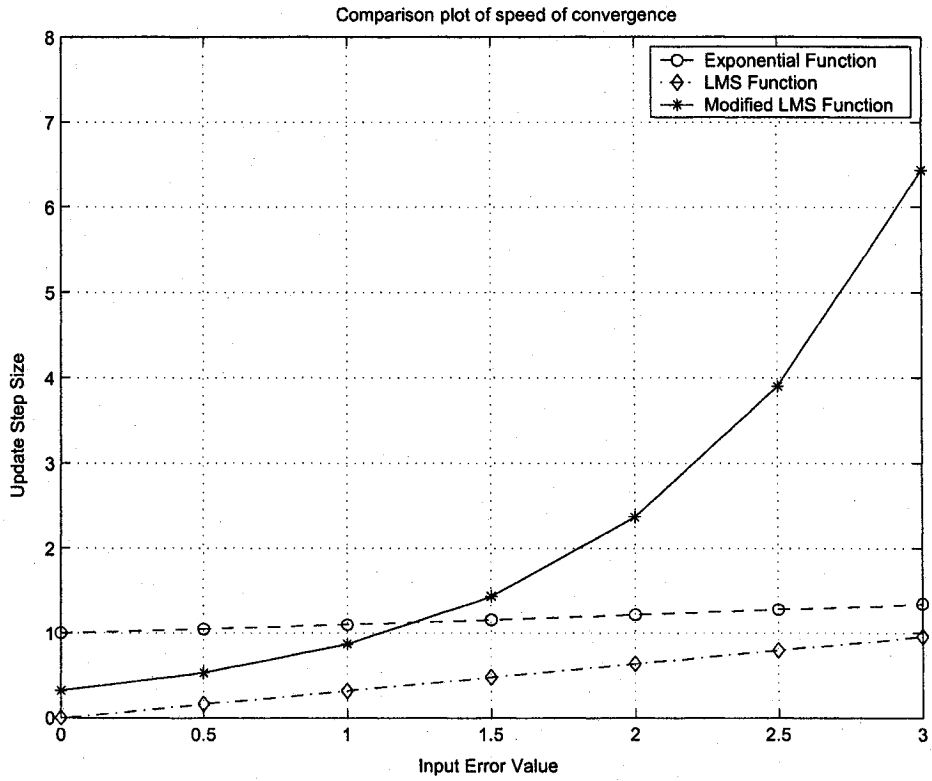

Figure 3.3: Plot of update step size against the error value for the LMS algorithm.

algorithm and modified LMS algorithm, $y = \mu x\xi$ and $y = \mu e^{\xi} x$, respectively. It can be seen from the figure that the modified LMS algorithm takes larger steps to achieve the target and thus converges faster.

3.6 SIR Estimation

In power control, accurate SIR estimation is also very much important to maintain the quality of the algorithm. A simple and effective SIR estimation scheme is proposed in [25]. In what follows, we highlight the main results from [25] that are relevant to

our work. The SIR at the receiver output is given by

$$\frac{S}{I+n} = \frac{\mu^2}{\bar{I}(k)}, \tag{3.4}$$

where S is the signal power, I is the interference power, n is the noise power, $\bar{I}(k)$ is the long-term interference plus the noise measurement for the kth iteration and μ is the mean of the ns despread symbols and is given by

$$\mu = \frac{1}{ns}\sum_{i=1}^{ns} |x_i| . \tag{3.5}$$

Let $\sigma^2(k)$ represent the instantaneous interference plus the noise power measurement in the kth iteration. This short term measurement is thus given as

$$\sigma^2(k) = \frac{1}{ns}\sum_{i=1}^{ns} |x_i|^2 - \mu^2. \tag{3.6}$$

$\sigma^2(k)$ is used to estimate $\bar{I}(k)$ given by (3.6) and follows from the definition of variance. To estimate $\bar{I}(k)$ from $\sigma^2(k)$, a moving average filter of window length L is used as

$$\bar{I}(k) = \sum_{i=0}^{L-1} \frac{\sigma^2(k-i)}{L}. \tag{3.7}$$

It has been observed in [25] that the mean and variance of the error increase with decreasing ns as well as decreasing SNR. From this point of view, it is appropriate to perform SIR estimation after RAKE combining since the output of the RAKE would

have a higher SNR.

3.7 Convergence Analysis

We show in this section that the proposed SIR-based algorithm converges to a fixed point. We know that the power control algorithm

$$p(n+1) = T\left(p(n)\right) \tag{3.8}$$

converges to a fixed point, denoted by p^*, where $p = [P_1, P_2, \ldots, P_U]$ is the transmit power vector. This convergence takes place provided that $T(p)$ is a standard interference function, i.e., the function should satisfy following conditions defined in [31].

- Positivity: $T(p) > \mathbf{0}$ where $\mathbf{0}$ is a zero vector of length U.
- Scalability: For all $\alpha > 1$, $\alpha T(p) > T(\alpha p)$.
- Monotonicity: If $p \geq p'$, then $T(p) \geq T(p')$.

The fixed point p^* also has the property that $p^* \leq s$ for all s. In addition, the above conditions also imply the convergence of the algorithm in (3.8).

We now show that these 3 conditions are satisfied when $T(p)$ is as defined by (3.2) and (3.3). We now examine each condition.

1. Positivity

Let us assume that $T_i(p(n)) = P_i(n) \cdot e^{(\mathrm{SIR_{tgt}} - \mathrm{SIR_{est}}(p_i(n)))} \cdot \mu \cdot \mathrm{SIR_{est}}(p_i(n))$ which is the case for the condition $\mathrm{SIR_{tgt}} - \mathrm{SIR_{est}}(p_i(n)) > 0$. ($\mathrm{SIR_{est}}(p_i(n))$ is equivalent to $\mathrm{SIR}^i_{\mathrm{est}}$ defined before, except the former definition is for a particular iteration and it clearly shows its dependence on the power of ith user.) We can say that as long as the SIR criterion is satisfied, the value of $T_i(p(n))$ is always going to be positive. Similarly, when $\mathrm{SIR_{tgt}} - \mathrm{SIR_{est}}(p_i(n)) < 0$, (3.3) will always give a positive value as long as the adaptation parameter μ is positive. Thus, we can say that the algorithm under consideration is positive in both cases.

2. Scalability

Let us consider $\mathrm{SIR_{tgt}} - \mathrm{SIR_{est}}(p_i(n)) > 0$. In this case, $T_i(p(n)) = P_i(n) \cdot e^{(\mathrm{SIR_{tgt}} - \mathrm{SIR_{est}}(p_i(n)))} \cdot \mu \cdot \mathrm{SIR_{est}}(p_i(n))$.

Now, for this algorithm to satisfy the scalability property, we need to show that $\alpha T_i(p(n)) > T_i(\alpha p(n))$ for all $\alpha > 1$.

$$\alpha T_i(p(n)) = \alpha \cdot P_i(n) \cdot e^{(\mathrm{SIR_{tgt}} - \mathrm{SIR_{est}}(p_i(n)))} \cdot \mu \cdot \mathrm{SIR_{est}}(p_i(n)) \tag{3.9}$$

and

$$T_i(\alpha p(n)) = \alpha \cdot P_i(n) \cdot e^{(\mathrm{SIR_{tgt}} - \mathrm{SIR_{est}}(\alpha p_i(n)))} \cdot \mu \cdot \mathrm{SIR_{est}}(\alpha p_i(n)). \tag{3.10}$$

As the power increases, the corresponding SIR value will increase accordingly.

Thus we can say that $\text{SIR}_{\text{est}}(\alpha p_i(n)) \geq \text{SIR}_{\text{est}}(p_i(n))$. Here, the exponential term $e^{(\text{SIR}_{\text{tgt}} - \text{SIR}_{\text{est}}(\alpha p_i(n)))}$ in (3.10) will try to reduce the value of $T_i(\alpha p(n))$ compared to $\alpha T_i(p(n))$. But, the term $\text{SIR}_{\text{est}}(\alpha p_i(n))$ in (3.10) will increase the value of $T_i(\alpha p(n))$. Here, since the term $e^{(\text{SIR}_{\text{tgt}} - \text{SIR}_{\text{est}}(\alpha p_i(n)))}$ will reduce the value of $T_i(\alpha p(n))$ exponentially which is faster as compared to the linear increment by $\text{SIR}_{\text{est}}(\alpha p_i(n))$, the former term will dominate the the latter one, resulting in a reduction in $T_i(\alpha p(n))$. Thus from (3.9) and (3.10), we can conclude that $\alpha T_i(p(n)) > T_i(\alpha p(n))$ for all $\alpha > 1$.

Now, consider the case $\text{SIR}_{\text{tgt}} - \text{SIR}_{\text{est}}(p_i(n)) < 0$. In this case, $T_i(p) = P_i(n) \cdot \frac{1}{e^{(\text{SIR}_{\text{est}}(p_i(n)) - \text{SIR}_{\text{tgt}}) \cdot \mu \cdot \text{SIR}_{\text{est}}(p_i(n))}}$. Then we can write

$$\alpha T_i(p(n)) = \frac{\alpha \cdot P_i(n)}{e^{(\text{SIR}_{\text{est}}(p_i(n)) - \text{SIR}_{\text{tgt}}) \cdot \mu \cdot \text{SIR}_{\text{est}}(p_i(n))}} \tag{3.11}$$

and

$$T_i(\alpha p(n)) = \frac{\alpha \cdot P_i(n)}{e^{(\text{SIR}_{\text{est}}(\alpha p_i(n)) - \text{SIR}_{\text{tgt}}) \cdot \mu \cdot \text{SIR}_{\text{est}}(\alpha p_i(n))}}. \tag{3.12}$$

Since $\text{SIR}_{\text{est}}(\alpha p_i(n)) \geq \text{SIR}_{\text{est}}(p_i(n))$, we can easily conclude from (3.11) and (3.12) that $\alpha T_i(p(n)) > T_i(\alpha p(n))$ for any value of $\alpha > 1$. So the proposed algorithm satisfies the scalability property.

3. Monotonicity

To prove that the algorithm is monotonic, we need to show that

$$\frac{\partial T_i\left(p(n)\right)}{\partial P_j(n)} \geq 0 \qquad \forall i, j. \tag{3.13}$$

Let us consider the case when $\mathrm{SIR}_{\mathrm{tgt}} - \mathrm{SIR}_{\mathrm{est}}(p_i(n)) > 0$.

$$T_i(p(n)) = P_i(n) \cdot e^{(\mathrm{SIR}_{\mathrm{tgt}} - \mathrm{SIR}_{\mathrm{est}}(p_i(n)))} \cdot \mu \cdot \mathrm{SIR}_{\mathrm{est}}(p_i(n)). \tag{3.14}$$

The estimated SIR at the receiver end can be defined as

$$\mathrm{SIR}_{\mathrm{est}}(p_i(n)) = \frac{G_{ii}P_i(n)}{\sum_{j \neq i} G_{ij}P_j(n) + N_0 W}. \tag{3.15}$$

where W is the total bandwidth, N_0 is the noise spectral density, and G_{ij} represents the gain between the jth mobile and the base station corresponding to the ith user and $Q(x) = \frac{1}{\sqrt{2\pi}} \int_x^\infty e^{-t^2/2} dt$.

Consider the case when $i \neq j$. As $P_j(n)$ increases, total interference in the system increases and it can be observed from (3.15) that the value of the $\mathrm{SIR}_{\mathrm{est}}(p_i(n))$ at the intended user degrades. Degradation in the $\mathrm{SIR}_{\mathrm{est}}(p_i(n))$ ultimately increases the value of $e^{(\mathrm{SIR}_{\mathrm{tgt}} - \mathrm{SIR}_{\mathrm{est}}(p_i(n)))}$, and thus increasing the transmit power $P_i(n)$. So we can say that

$$\frac{\partial T_i\left(p(n)\right)}{\partial P_j(n)} > 0, \qquad \text{for } i \neq j. \tag{3.16}$$

We now consider the case when $i = j$. Here we will have to evaluate the value of $\partial T_i(p(n))/\partial P_i(n)$. Thus, we can write

$$\begin{aligned}
\frac{\partial T_i(p(n))}{\partial P_i(n)} &= \frac{\partial}{\partial P_i(n)} \left(P_i(n) \cdot e^{(\mathrm{SIR}_{\mathrm{tgt}} - \mathrm{SIR}_{\mathrm{est}}(p_i(n)))} \cdot \mu \cdot \mathrm{SIR}_{\mathrm{est}}(p_i(n)) \right) \\
&= \mu \cdot \left\{ \begin{array}{c} e^{(\mathrm{SIR}_{\mathrm{tgt}} - \mathrm{SIR}_{\mathrm{est}}(p_i(n)))} \mathrm{SIR}_{\mathrm{est}}(p_i(n)) \\ + P_i(n) \mathrm{SIR}_{\mathrm{est}}(p_i(n)) \frac{\partial}{\partial P_i(n)} (e^{(\mathrm{SIR}_{\mathrm{tgt}} - \mathrm{SIR}_{\mathrm{est}}(p_i(n)))}) \\ + P_i(n) e^{(\mathrm{SIR}_{\mathrm{tgt}} - \mathrm{SIR}_{\mathrm{est}}(p_i(n)))} \frac{\partial}{\partial P_i(n)} (\mathrm{SIR}_{\mathrm{est}}(p_i(n))) \end{array} \right\} \\
&= \mu \cdot \left\{ \begin{array}{c} e^{(\mathrm{SIR}_{\mathrm{tgt}} - \mathrm{SIR}_{\mathrm{est}}(p_i(n)))} \mathrm{SIR}_{\mathrm{est}}(p_i(n)) \\ + P_i(n) \mathrm{SIR}_{\mathrm{est}}(p_i(n)) (-e^{(\mathrm{SIR}_{\mathrm{tgt}} - \mathrm{SIR}_{\mathrm{est}}(p_i(n)))} \cdot \frac{G_{ii}}{I_i}) \\ + P_i(n) e^{(\mathrm{SIR}_{\mathrm{tgt}} - \mathrm{SIR}_{\mathrm{est}}(p_i(n)))} \frac{G_{ii}}{I_i} \end{array} \right\} \\
&= \mu \cdot \left\{ \begin{array}{c} e^{(\mathrm{SIR}_{\mathrm{tgt}} - \mathrm{SIR}_{\mathrm{est}}(p_i(n)))} \mathrm{SIR}_{\mathrm{est}}(p_i(n)) \\ + P_i(n) e^{(\mathrm{SIR}_{\mathrm{tgt}} - \mathrm{SIR}_{\mathrm{est}}(p_i(n)))} \frac{G_{ii}}{I_i} (1 - \mathrm{SIR}_{\mathrm{est}}(p_i(n))) \end{array} \right\} \qquad (3.17)
\end{aligned}$$

It can be observed from (3.17) that increase in the value of $P_i(n)$ increase the value of the right hand side term in (3.17). Thus,

$$\frac{\partial T_i(p(n))}{\partial P_i(n)} = \mu \cdot \left\{ \begin{array}{c} e^{(\mathrm{SIR}_{\mathrm{tgt}} - \mathrm{SIR}_{\mathrm{est}}(p_i(n)))} \mathrm{SIR}_{\mathrm{est}}(p_i(n)) \\ + P_i(n) e^{(\mathrm{SIR}_{\mathrm{tgt}} - \mathrm{SIR}_{\mathrm{est}}(p_i(n)))} \frac{G_{ii}}{I_i} (1 - \mathrm{SIR}_{\mathrm{est}}(p_i(n))) \end{array} \right\} > 0.$$

The same can also be derived and concluded for the case when $\mathrm{SIR}_{\mathrm{tgt}} - \mathrm{SIR}_{\mathrm{est}}(p_i(n)) < 0$. Hence the algorithm satisfies all three necessary conditions for convergence.

3.8 Simulation Results

In this section, we present the comparison results for the following three algorithms: 1) the 3GPP Standard Algorithm 1 [8], 2) the exponential update function algorithm [13], and 3) the SIR-based proposed algorithm. The system considered in this study is same as that of the proposed uplink model of FDD WCDMA [7] – [9]. Power Control is only applied at Layer 1 (i.e. inner closed loop power control). The channel model is considered to be a frequency selective Rayleigh fading channel with l paths. The fading channel is assumed to be changing per frame. The power delay profile is assumed to be uniform.

The noise is modelled as additive white gaussian noise (AWGN). The target SIR is fixed to 4 dB. The SIR at the receiver end is measured on the DPDCH instead of DPCCH as proposed in [25]. During the simulations, we assume five different users ready to transmit data and the data is received at the base station through three different transmission paths. The transmitter and the receiver structure in the uplink direction considered is as shown in Fig. 2.1. Closed loop power control is taken into consideration as shown in Fig. 3.1. The UEs are assumed to be mobile with different Doppler frequencies taken into consideration. This simulates the algorithm for different mobile speeds. A carrier frequency of 1940 MHz is assumed for calculating the Doppler frequency. The Doppler frequency is normalized to 1500 Hz, i.e., to the power control frequency. The carrier frequency is related to the Doppler frequency

by the relation

$$f_d = f_c \times \frac{v}{c}, \tag{3.18}$$

where f_d is the Doppler frequency, f_c is the carrier frequency, v is the velocity of the mobile device and c is the speed of light which is 3×10^8 m/s.

We also chose the frame format and the number of bits detail from [7]. In the downlink direction, slot format number 14 [7] is used ($N_{Data1} = 56, N_{Data2} = 232, N_{TPC} = 8, N_{Pilot} = 16$). A maximum limit on the transmit power is also considered. Call dropping and admission control is not considered in our simulation.

In Fig. 3.4, we show a comparison plot of the 3GPP PCA1 and the proposed algorithm. The figure is plotted with estimated SIR against the iteration index. This plot mainly compares the speed of convergence. It can be observed that the 3GPP PCA1 converges very slowly as compared to the proposed algorithm and thus takes more time to stabilize. We also observe from the figure that, as the value of μ decreases, the speed of convergence increases giving rise to instabilities in the estimated SIR value. Thus, it is very important to make a proper choice of μ as per the requirement.

Fig. 3.5 shows the magnified version of the Fig. 3.4. It clearly shows the convergence speed of different algorithms. It can be observed that the 3GPP proposed algorithm 1 takes almost 15 iterations to converge to the target value. But in the same time, the proposed algorithm takes less time to converge.

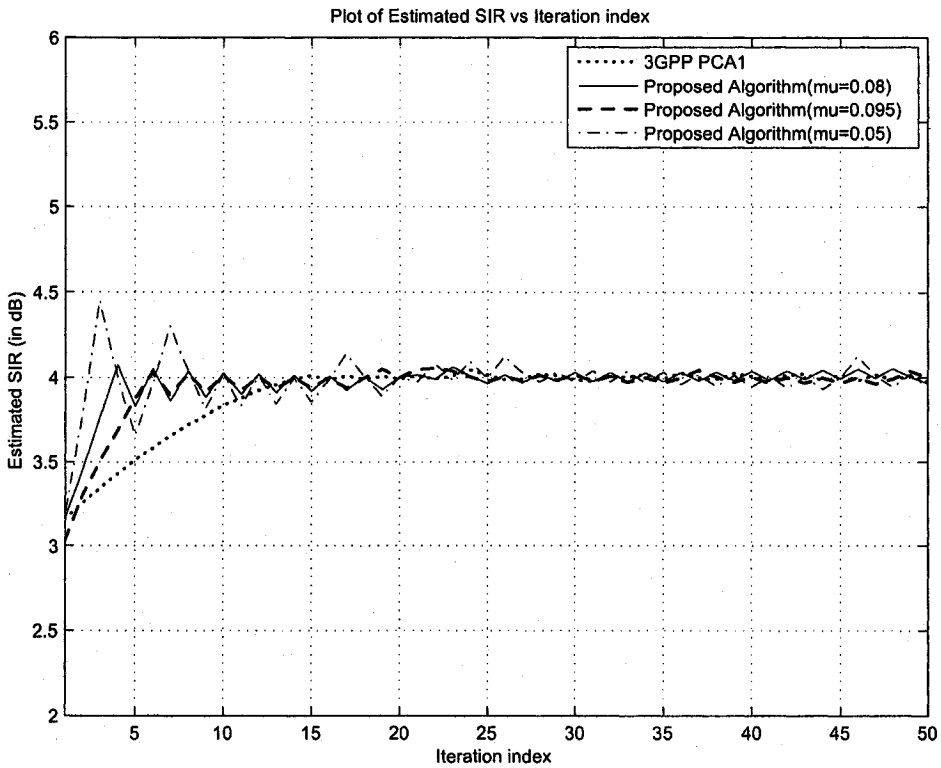

Figure 3.4: Comparison plot between 3GPP algorithm and SIR-based proposed algorithm.

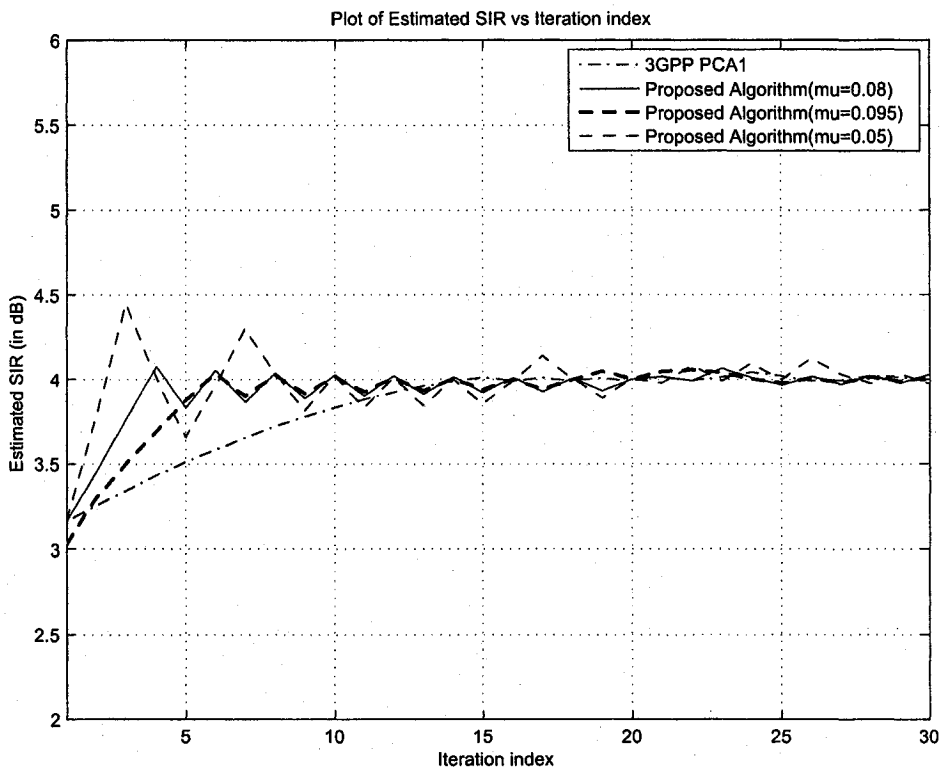

Figure 3.5: Comparison plot between 3GPP and SIR-based proposed algorithm (magnified version).

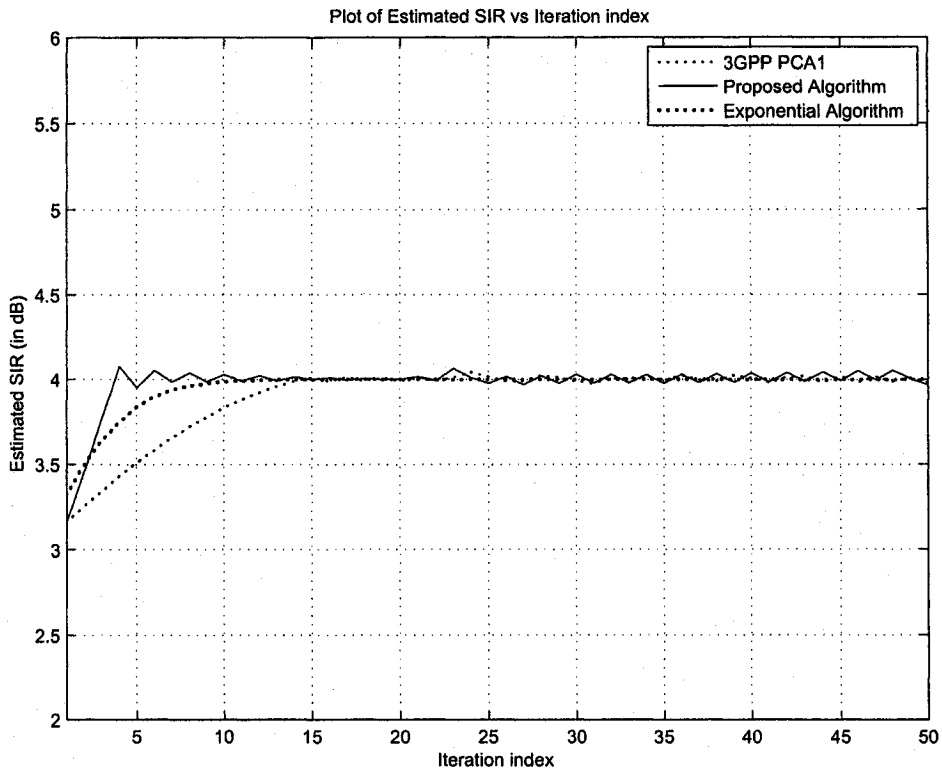

Figure 3.6: Comparison plot for the three algorithms.

Fig. 3.6 shows a comparison between the 3GPP algorithm, the exponential function algorithm and the proposed algorithm. In this case, we set the μ value equal to 0.08. It can be seen from the figure that the proposed algorithm converges faster as compared to the other two algorithms. The variation in the estimated SIR in the convergence period can be assumed to be within a tolerable range and thus can be assumed to be stabilized. The magnified version of Fig. 3.6 is shown in Fig. 3.7, which explains the exact convergence comparison between the three algorithms.

In Fig. 3.8, we see the response of the proposed algorithm to changes in $\mathrm{SIR_{tgt}}$ made during the simulation period. The $\mathrm{SIR_{tgt}}$ is first set to 4 dB for until the

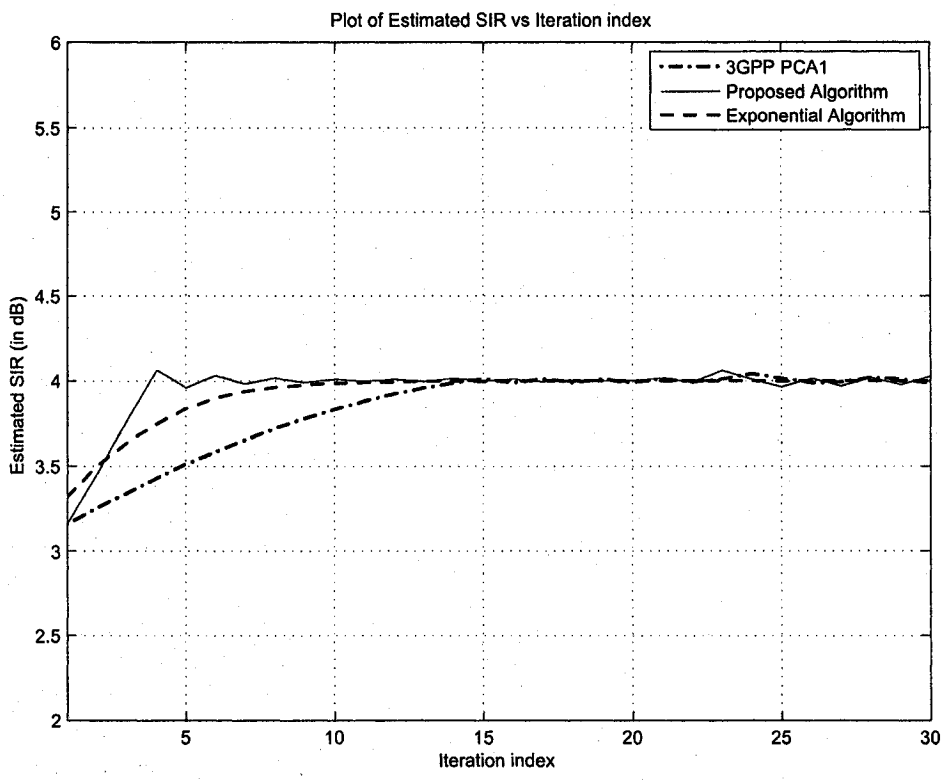

Figure 3.7: Comparison plot for the algorithms under consideration (magnified version).

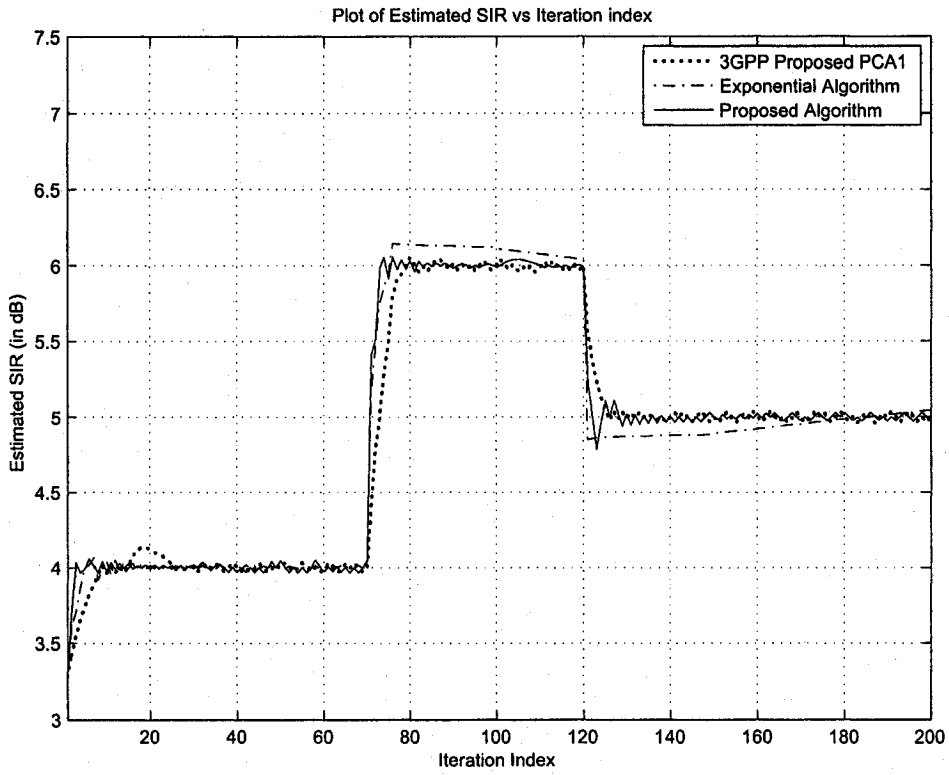

Figure 3.8: Plot showing response of the SIR-based proposed algorithm to the changes in the SIR_{tgt} value.

algorithm converges, and is then set to 6 dB until the algorithm converges again, and is finally set to 5 dB. It is clear from the figure how robust the proposed algorithm in tracking the variation in the target SIR.

Fig. 3.9 presents a comparison plot among the cases with different simultaneous user numbers for the proposed algorithm. Increase in the user number increases the interference in the cellular system. It can be seen from the figure that an increase in the number of users takes more number of iterations to achieve the desired value. We can also say that increase in the interference level also increases the average required

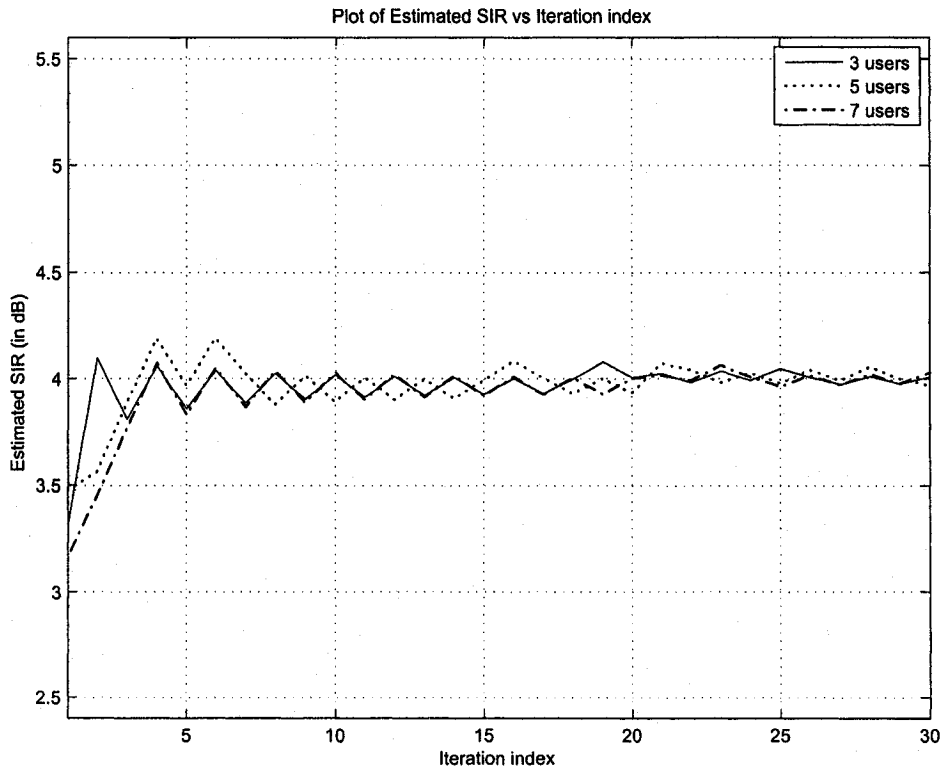

Figure 3.9: Plot of estimated SIR with different number of users for the proposed algorithm.

SNR value.

Fig. 3.10 compares between the three power control algorithms based on the average value of SNR required. The adaptation parameter μ is fixed to 0.08 during the simulation. This simulation considers the UE at different velocities by considering different doppler frequencies. The gain in SNR is between 1.0. to 1.5 dB over the 3GPP algorithm and about 1.0 dB over the exponential algorithm. This achieved gain proves the capacity of the proposed algorithm to manage the available resources properly.

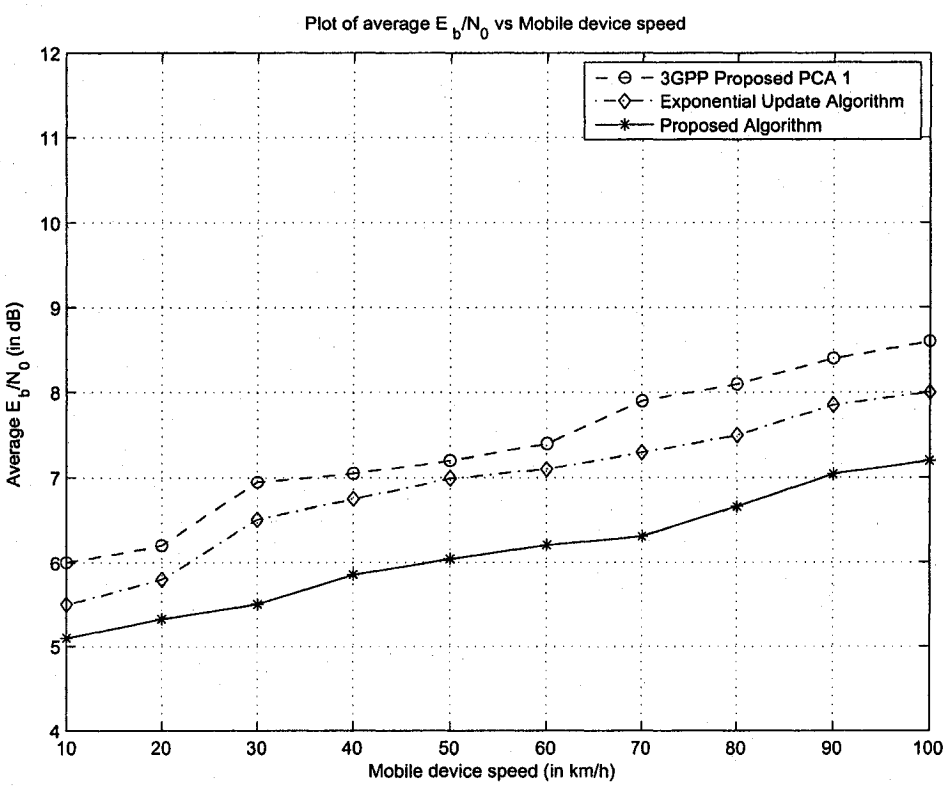

Figure 3.10: Comparison graph with E_b/N_0 as the parameter.

3.9 Conclusion

In this chapter, we took a look at few of previously proposed power control algorithms. We proposed a distributive first order power control algorithm which contains a modified LMS power update function. The algorithm takes lesser time to reach to the target value as compared to the 3GPP proposed fixed step algorithm and the exponential function algorithm [13]. Decreasing the value of adaptation parameter μ increases the convergence speed, increasing the variations in the settling phase.

Observing the comparison graphs, we can say that the average required SNR for the proposed algorithm is less as compared to the other two algorithms. This implies a gain in the required SNR and thus, increases the capacity of the network making proper utilization of the system resources. The gain in SNR is around 0.5 to 1 dB.

Chapter 4

Proposed BER-Based Power Control Algorithm

4.1 Introduction

In this chapter, we propose an efficient BER-based power control algorithm for WCDMA systems. As we know, BERs and transmit powers are not linearly related, but rather BER is more of an exponential function of powers [29]. Since the natural logarithmic function is the inverse of the exponential function, it makes sense to use the former function in the proposed algorithm for power updating. It is also known that the natural logarithmic function converges faster compared to the base-10 logarithmic function, which again motivates the use of this function to achieve faster convergence. We analyze the proposed algorithm in terms of its convergence and show that it always converges. We demonstrate that the proposed algorithm

converges faster than existing BER-based algorithms and results in reducing the required SNR to achieve a certain system performance. We also demonstrate that the proposed algorithm is robust against high mobile speeds.

4.2 System Model

The system model followed here is the same as discussed in Section 3.2. The user data bits and control information are present on the dedicated channels DPDCH and DPCCH, respectively. As shown in Fig. 3.1, data of the UE is spread and processed according to the WCDMA standards. After complete demodulation and despreading, BER is estimated using already known pilot symbol pattern. According to the measured and desired value of BER, a power control command is transmitted from the BS to the UE. The command is decoded using a command decoder at the UE. According to the "power up" or "power down" command, power is updated and the UE transmits with the updated power. Thus a feedback power control loop is maintained.

4.3 BER-Based Proposed Algorithm

Here we also assume that there are U users. Let BER_{tgt} denote the target BER, i.e., data transmission reliability, and let BER_i denote the measured BER for user i. In order to achieve the BER_{tgt} with minimum transmit power, we propose a power control algorithm which utilizes the measured and target bit error rate to update the

transmit power of the UE. Let BER_i denotes the received BER value of the ith user and BER_{tgt} denotes the target value of the BER. Let Δ_2^i be the difference between the target BER and the received BER for the ith user, (BER_i). The power update at the $(n+1)$th iteration can be given as follows.

If $\Delta_2^i < 0$,

$$P_i(n+1) = P_i(n) \cdot \ln\left(\frac{e^{\mu} \cdot \text{BER}_i}{\text{BER}_{\text{tgt}}}\right), \tag{4.1}$$

else if $\Delta_2^i > 0$,

$$P_i(n+1) = \frac{P_i(n)}{\ln\left(\frac{e^{\mu} \cdot \text{BER}_{\text{tgt}}}{\text{BER}_i}\right)}, \tag{4.2}$$

where μ is the adaptation parameter. (There is no power update when $\Delta_2^i = 0$.) As can be seen from (4.1) and (4.2), only a single previous sample is used for power update. Thus, this algorithm is a first order algorithm. Also, since there is no need to save the large database centrally, which makes the algorithm distributed.

4.4 Convergence Analysis

We show in this section that the proposed BER-based algorithm converges to a fixed point p^*. The general relation between BER and power can be written as

$$\text{BER}_i(p(n)) = Q\left(\sqrt{\frac{mG_{ii}P_i(n)}{\sum_{j\neq i} G_{ij}P_j(n) + N_0W}}\right), \tag{4.3}$$

where m is a constant the value of which depends upon the type of modulation used at the transmitter.

Now, we will prove the convergence of the proposed algorithm. The algorithm can be expressed as

$$p(n+1) = T\left(p(n)\right). \tag{4.4}$$

If there exists a power vector s that meets the desired SIR requirement of all the users, i.e.,

$$\mathrm{BER}_j(s) \geq B_j, \ \forall j, \tag{4.5}$$

then if the algorithm in (4.4) satisfies the three necessary conditions for convergence, the algorithm is said to converge to a unique fixed point, p^*. The fixed point p^* has the property that $p^* \leq s$ for all s which satisfy (4.5).

We now show that these three conditions are satisfied when $T(p)$ is as defined by (4.1) and (4.2). We now examine each condition.

1. Positivity

   We know that achieved BER can be expressed as [32]

$$\mathrm{BER}_i = Q\left(\sqrt{m \cdot \mathrm{SIR}_i}\right), \tag{4.6}$$

where m is a constant and SIR_i is given as

$$\text{SIR}_i = \frac{mG_{ii}P_i}{\sum_{j\neq i} G_{ij}P_j + N_0 W}. \tag{4.7}$$

When $\text{BER}_{\text{tgt}} - \text{BER}_i(p(n)) < 0$, (4.1) is always positive. Similarly, when $\text{BER}_{\text{tgt}} - \text{BER}_i(p(n)) > 0$, (4.2) will always be positive. Thus, we can say that the algorithm under consideration is positive in both cases.

2. Scalability

To prove the scalability, let us consider the case when $\text{BER}_{\text{tgt}} - \text{BER}_i(p(n)) < 0$. In this condition, $T_i(p(n)) = P_i(n) \cdot \ln\left(\frac{e^{\mu}\cdot \text{BER}_i(p(n))}{\text{BER}_{\text{tgt}}}\right)$. Thus

$$\begin{aligned} \alpha T_i(p(n)) &= \alpha \cdot P_i(n) \cdot \ln\left(\frac{e^{\mu}\cdot \text{BER}_i(p(n))}{\text{BER}_{\text{tgt}}}\right) \\ &= \alpha \cdot P_i(n) \cdot \ln\left(\frac{e^{\mu}\cdot Q\left(\sqrt{m\cdot \text{SIR}_i(p(n))}\right)}{\text{BER}_{\text{tgt}}}\right) \end{aligned} \tag{4.8}$$

and

$$\begin{aligned} T_i(\alpha p(n)) &= \alpha \cdot P_i(n) \cdot \ln\left(\frac{e^{\mu}\cdot \text{BER}_i(\alpha p(n))}{\text{BER}_{\text{tgt}}}\right) \\ &= \alpha \cdot P_i(n) \cdot \ln\left(\frac{e^{\mu}\cdot Q\left(\sqrt{m\cdot \text{SIR}_i(\alpha p(n))}\right)}{\text{BER}_{\text{tgt}}}\right). \end{aligned} \tag{4.9}$$

Here, for $\alpha > 1$, $\text{SIR}_i(\alpha p(n)) \geq \text{SIR}_i(p(n))$ and $Q(x)$ is a monotonically decreasing function. Thus, by comparing (4.8) and (4.9) we see that $\alpha T_i(p(n)) >$

$T_i(\alpha p(n))$. This can also be proved for the case $\text{BER}_{\text{tgt}} - \text{BER}_i(p(n)) > 0$.

3. Monotonicity

To show that the algorithm is monotonic, we show that

$$\frac{\partial T_i\left(p(n)\right)}{\partial P_j(n)} \geq 0 \qquad \forall i, j. \tag{4.10}$$

For the case $\text{BER}_{\text{tgt}} - \text{BER}_i(p(n)) < 0$, $T_i(p(n))$ can be formulated from (4.1) as

$$\begin{aligned} T_i(p(n)) &= P_i(n) \cdot \ln\left(\frac{e^{\mu} \cdot \text{BER}_i(p(n))}{\text{BER}_{\text{tgt}}}\right) \\ &= P_i(n) \cdot \ln\left(\frac{e^{\mu} \cdot Q\left(\sqrt{m \cdot \text{SIR}_i(p(n))}\right)}{\text{BER}_{\text{tgt}}}\right). \end{aligned} \tag{4.11}$$

Considering the case when $i \neq j$ and increasing $P_j(n)$, we can observe from (4.6) that the value of the achieved $\text{SIR}_i(p(n))$ at the intended user degrades. Since the Q-function is monotonically decreasing, a decrease in SIR_i increases the value of the term $Q\left(\sqrt{m \cdot \text{SIR}_i(p(n))}\right)$. Since the natural logarithmic function is monotonically increasing, an increase in the Q-function also increases the transmit power $P_i(n)$. Thus, we can say that

$$\frac{\partial T_i\left(p(n)\right)}{\partial P_j(n)} > 0, \qquad \text{for } i \neq j. \tag{4.12}$$

We now consider the case when $i = j$. Here we will have to evaluate the value

of $\partial T_i(p(n))/\partial P_i(n)$. In this case, $T_i(p(n)) = P_i(n) \cdot \ln\left(\frac{e^{\mu} \cdot \mathrm{BER}_i(p(n))}{\mathrm{BER}_{\mathrm{tgt}}}\right)$.

$$
\begin{aligned}
\frac{\partial T_i(p(n))}{\partial P_i(n)} &= \frac{\partial}{\partial P_i(n)}\left(P_i(n) \cdot \ln\left(\frac{e^{\mu} \cdot \mathrm{BER}_i(p(n))}{\mathrm{BER}_{\mathrm{tgt}}}\right)\right) \\
&= \frac{\partial}{\partial P_i(n)}\left(P_i(n) \cdot \ln\left(\frac{e^{\mu} \cdot Q\left(\sqrt{m \cdot \mathrm{SIR}_i(p(n))}\right)}{\mathrm{BER}_{\mathrm{tgt}}}\right)\right) \\
&= \ln\left(\frac{e^{\mu} \cdot Q\left(\sqrt{m \cdot \mathrm{SIR}_i(p(n))}\right)}{\mathrm{BER}_{\mathrm{tgt}}}\right) \\
&\quad + P_i(n) \cdot \frac{\partial}{\partial P_i(n)}\left(\ln\left(\frac{e^{\mu} \cdot Q\left(\sqrt{m \cdot \mathrm{SIR}_i(p(n))}\right)}{\mathrm{BER}_{\mathrm{tgt}}}\right)\right) \\
&= \ln\left(\frac{e^{\mu} \cdot Q\left(\sqrt{m \cdot \mathrm{SIR}_i(p(n))}\right)}{\mathrm{BER}_{\mathrm{tgt}}}\right) \\
&\quad + \left(\begin{array}{l} P_i(n) \cdot \frac{\mathrm{BER}_{\mathrm{tgt}}}{e^{\mu} \cdot Q\left(\sqrt{m \cdot \mathrm{SIR}_i(p(n))}\right)} \cdot \\ \frac{\partial}{\partial P_i(n)}\left(\frac{e^{\mu} \cdot Q\left(\sqrt{m \cdot \mathrm{SIR}_i(p(n))}\right)}{\mathrm{BER}_{\mathrm{tgt}}}\right) \end{array}\right) \\
&= \ln\left(\frac{e^{\mu} \cdot Q\left(\sqrt{m \cdot \mathrm{SIR}_i(p(n))}\right)}{\mathrm{BER}_{\mathrm{tgt}}}\right) \\
&\quad + \left(\begin{array}{l} \frac{P_i}{Q\left(\sqrt{m \cdot \mathrm{SIR}_i(p(n))}\right)} \cdot \frac{Q\left(\sqrt{m \cdot \mathrm{SIR}_i(p(n))}\right)}{\sqrt{4\pi}} \cdot \\ \frac{e^{-\mathrm{SIR}_i(p(n))}(1 - 2 \cdot \mathrm{SIR}_i(p(n)))}{2\sqrt{\mathrm{SIR}_i(p(n))}} \cdot \frac{G_{ii}}{I_i} \end{array}\right) \\
&= \ln\left(\frac{e^{\mu} \cdot Q\left(\sqrt{m \cdot \mathrm{SIR}_i(p(n))}\right)}{\mathrm{BER}_{\mathrm{tgt}}}\right) \\
&\quad + \left(\frac{\sqrt{\mathrm{SIR}_i(p(n))}}{\sqrt{16\pi}} \cdot e^{-\mathrm{SIR}_i(p(n))}(1 - 2 \cdot \mathrm{SIR}_i(p(n)))\right). \quad (4.13)
\end{aligned}
$$

In (4.13), as long as $\mathrm{BER}_{\mathrm{tgt}} - \mathrm{BER}_i(p(n)) < 0$, first term is always positive. The negative exponential factor in the second term keeps the value of the second term

very small. Thus, it can be easily concluded that $\partial T_i(p(n))/\partial P_i(n) \geq 0$. The same can also be derived and concluded for the case when $\text{BER}_{\text{tgt}} - \text{BER}_i(p(n)) > 0$. Hence the algorithm satisfies all three necessary conditions for convergence.

4.5 Simulation Results

We present the comparison results for the following three algorithms: 1) the 3GPP standard algorithm 1 (3GPP PCA1) [8], 2) the BER-based algorithm given in [29], and 3) our BER-based proposed algorithm. The system considered in this study is same as that of the proposed uplink model of FDD WCDMA [9]. Power control is applied only at layer 1 (i.e. inner closed loop power control). The channel model is considered to be a frequency selective Rayleigh fading channel with l paths. The fading channel is assumed to be changing per frame. The PDP is assumed to be uniform. The noise is modeled as AWGN.

The pilot bits on the DPCCH channel are known bits and thus can be used at the receiver end to calculate the bit error rate. Five pilot bits per slot have been chosen in the simulations. Note that, in a frame, every slot contains different sequences of zeros and ones and the frame content repeats. During the simulations, we assume five different users ready to transmit data and the data is received at the base station through four different transmission paths at relative delays of 0, 4, 8 and 12 chips. The transmitter and the receiver structure in the uplink direction considered is as shown in Figs. 2.1 (a) and (b), respectively. The UEs are assumed to be mobile with

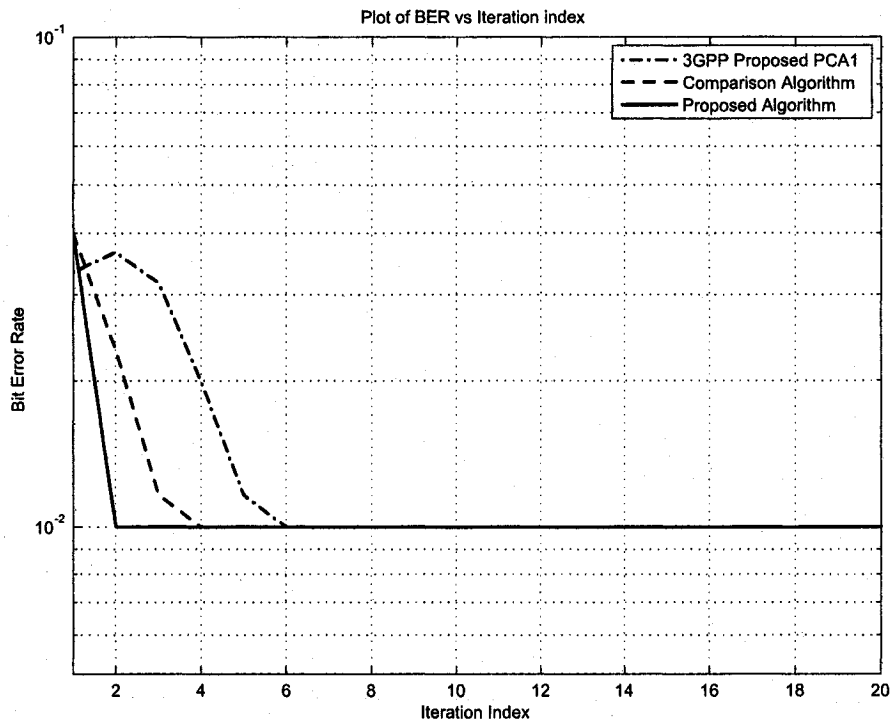

Figure 4.1: Plot of BER vs Iteration index for different algorithms with BER_{tgt} equals 10^{-2}.

a velocity of 10 km/h for all the simulation results. A carrier frequency of 1940 MHz is assumed for calculating the Doppler frequency. The Doppler frequency is normalized to 1500 Hz, i.e., to the power control frequency. Call dropping and admission control is not considered in our simulation.

In Fig. 4.1, we show a comparison plot of the 3GPP PCA1 and the proposed algorithm. The figure is plotted with measured BER against the iteration index. The BER_{tgt} is set to 10^{-2} with $\mu = 0.4$. It can be observed that the 3GPP PCA1 converges very slowly as compared to the proposed algorithm and thus takes more time to stabilize.

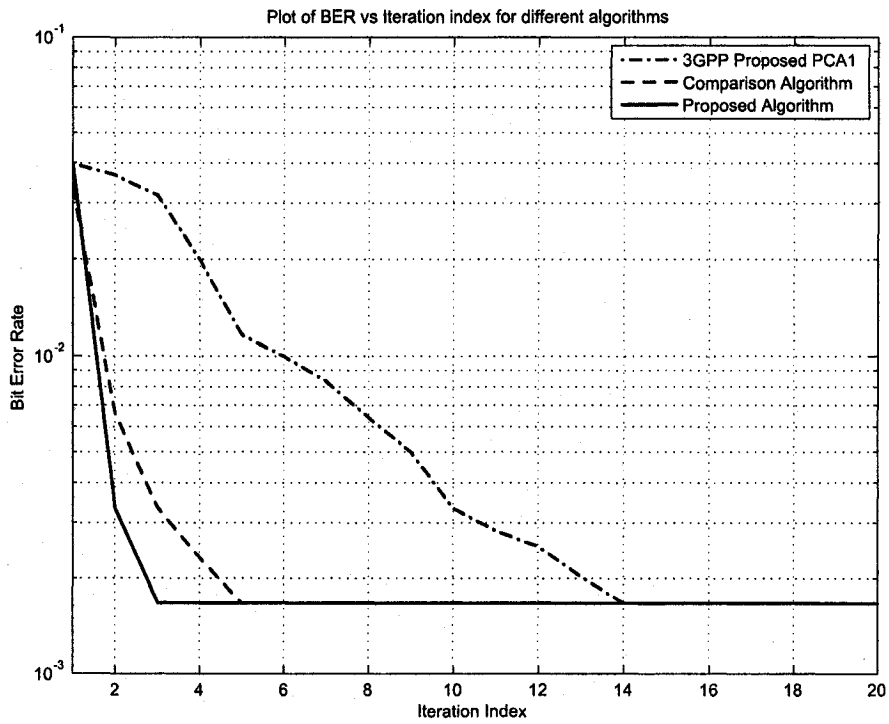

Figure 4.2: Plot of BER vs iteration index for different algorithms with BER_{tgt} equals 2×10^{-3}.

Fig. 4.2 again shows a comparison between the three power control algorithms under consideration. Here, we set $\mu = 0.4$ and BER_{tgt} is set to 2×10^{-3}. It can be observed that the proposed algorithm converges faster than both algorithms. Thus the proposed algorithm is quicker in response and follows the changes in transmission medium quickly.

Fig. 4.3 compares between the three power control algorithms based on the average value of SNR required. The adaptation parameter μ is fixed to 0.4 during the simulation. This simulation considers the UE at different velocities by considering different Doppler frequencies. The gain in SNR is between 0.5 to 1.0 dB over the other

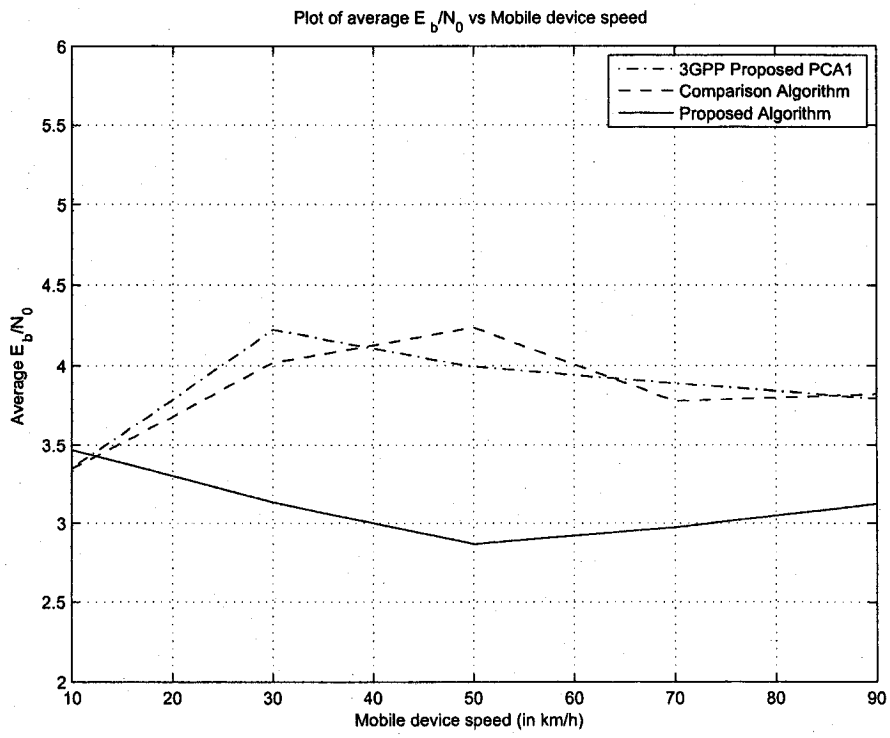

Figure 4.3: Plot of average SNR for different speeds of the UE.

two algorithms. This achieved gain proves the efficacy of the proposed algorithm to manage the available resources properly.

4.6 Conclusion

We proposed a BER-based power control algorithm that utilizes the natural logarithmic function in the power update process. The proposed algorithm is distributed and utilizes only a single previous sample for power update. We have shown that the convergence of the algorithms is guaranteed. We demonstrated that the proposed

algorithm converges faster than existing algorithms, including the 3GPP PCA1 BER-based algorithm [29]. We also demonstrated that the proposed algorithm reduces the required SNR to achieve a certain target BER at various mobile speeds.

Chapter 5

Conclusions and Future Work

5.1 Conclusions

In this thesis, we presented two distributed first order power control algorithms. SIR and BER are used as the decision criteria in two different power update functions. The non-linearity of the LMS algorithm resulting by incorporating an exponential function into the LMS algorithm helps to improve the speed of convergence of the proposed algorithm. The SIR-based algorithm achieves faster convergence to the desired value compared to the 3GPP PCA1 and the exponential update algorithms. It is also demonstrated to achieve a gain in the average required SNR value by this proposed algorithm. The SIR-based and BER-based algorithms are mathematically analyzed and their convergence is guaranteed. The proposed BER-based algorithm incorporates the natural logarithmic function which helps to achieve the near exact relationship between the BER and the transmit power. A superior performance in

terms of speed of convergence is illustrated by the BER-based algorithm compared to the 3GPP PCA1 and a previous BER-based algorithm. It can be observed that the algorithm uses already known pilot symbols for BER measurement and thus can be categorized as a deterministic algorithm. The BER-based algorithm achieves a gain in the average required SNR value over other algorithms under comparison. The robustness of these two proposed algorithms in the high mobility environment has also been shown.

5.2 Future Work

During the simulations, the loop delays are not taken into account. Considering loop delays in these closed loop power control algorithms will be a good extension to examine the robustness of the proposed algorithms in more details. Also when a UE is near the cell boundaries, soft handover comes into action and helps to combine the received signals from more than single BSs. Soft handover also takes care of combining of the power control commands received from different BSs. Thus in the future, it will be interesting to consider the working of the power control algorithms in soft handover environment.

Bibliography

[1] D. Magill, F. Natali, and G. Edwards, "Spread-spectrum technology for commercial applications," *Proc., IEEE,* vol. 82, issue 4, pp. 572-584, April 1994.

[2] T. Ojanpera and R. Prasad, "An overview of third-generation wireless personal communications: a European perspective," *IEEE transaction on Personal Communications,* vol.5, pp.59-65, Dec. 1998.

[3] H. Holma and A. Toskala, *WCDMA for UMTS*, John Wiley and Sons Inc., 2000.

[4] D. M. Novakovic and M. L. Dukic, "Evolution of the power control techniques for DS-CDMA towards 3G wireless communication systems," *IEEE Commun. Surveys*, vol. 3, no. 4, 4^{th} Quarter 2000.

[5] F. Adachi, M. Sawahashi, and K. Okawa, "Tree-structured generation of orthogonal spreading codes with different lengths for forward link of DS-CDMA mobile radio," *Electronics Letters*, vol. 33, no. 1, pp. 27-28, Jan. 1997.

[6] TSG RAN Working Group 1 meeting no. 18, *Performance comparison of SIR based and level based UL Power control in case of Fading AWGN Interference.*

[7] 3^{rd} Generation Partnership Project, Technical Specification Group Radio Access Network, *Physical Channels and Mapping of Transport Channels onto Physical Channels (FDD) (Release 6)*, 3GPP TS 25.211 v6.2.0 (2004-09).

[8] 3^{rd} Generation Partnership Project, Technical Specification Group Radio Access Network, *Physical Layer Procedures (FDD) (Release 6)*, 3GPP TS 25.214 v6.3.0 (2004-09).

[9] 3^{rd} Generation Partnership Project, Technical Specification Group Radio Access Network, *Spreading and Modulation (FDD) (Release 6)*, 3GPP TS 25.213 v6.0.0 (2003-12).

[10] S. Ariyavisitakul and L. F. Chang, "Signal and interference statistics of a CDMA system with feedback power control," *IEEE Trans. Commun.*, vol. 41, no. 11, pp. 1626-1634, Nov. 1993.

[11] S. Ariyavisitakul, "SIR-based power control in a CDMA system," *Proc., IEEE GLOBECOM*, vol. 2, pp. 868-873, Dec. 1992.

[12] Y. J. Yang and J. F. Chang, "A strength-and-SIR-combined adaptive power control for CDMA mobile radio channels," *IEEE Trans. Veh. Techn.*, vol. 48, no. 6, pp. 1996-2004, Nov. 1999.

[13] L. Lv, S. Zhu, and Y. Wang, "A distributed power control algorithm for Wide-band CDMA cellular mobile systems," *Proc., IEEE Commun. Techn. Conf.*, vol.1, pp. 954-957, Aug. 2000.

[14] L. Lv, S.Zhu, and S. Dong, "Fast convergence distributed power control algorithm for WCDMA systems," *IEE Proc. Commun.*, vol.150, no. 2, pp. 134-140, April 2003.

[15] M. Rintamaki, I. Virtej, and H. Koivo, "Two-mode fast power control for WCDMA systems," *Proc., IEEE Veh. Techn. Conf.*, pp. 2893-2897, May 2001.

[16] M. Rintamaki, H. Koivo, and I. Hartimo, "Adaptive closed loop power control algorithms for CDMA cellular communication systems," *IEEE Trans. Veh. Techn.*, vol. 53, no. 6, pg. 1756-1768, Nov. 2004.

[17] S. Grandhi and J. Zander, "Constrained power control in cellular radio systems," *Proc., IEEE Veh. Techn. Conf.*, pp. 824-828, June 1994.

[18] R. Jantti and S. Kim, "Second-order power control with asymptotically fast convergence," *IEEE J. Selected Areas in Commun.*, vol. 18, no. 3, pp. 447-457, March 2000.

[19] M. Subramaniam and A. Anpalagan, "A pilot power based power control (PPBPC) and base station assignment algorithm in cellular CDMA networks," *Proc., IEEE Canadian Conference on Electrical and Computer Engineering*, vol. 1, pp. 327-332, May 2004.

[20] M. Elmusrati, M. Rintamäki, I. Hartimo, and H. Koivo, "Fully distributed power control algorithm with one bit signaling and nonlinear error estimation," *Proc., IEEE Veh. Technol. Conf.*, vol. 2, pp. 727-731, Oct. 2003.

[21] S. Naghian, M. Rintamäki and R. Baghaie, "Dynamic step-size power control in UMTS," *Proc., IEEE International Symposium on Personal, Indoor and Mobile Radio Communications*, vol. 4, pp. 1606-1610, Sept. 2002.

[22] J. Nasreddine, L. Nuaymi and X. Lagrange, "Downlink adaptive power control algorithm for 3G cellular CDMA networks," *Proc., IEEE International Symposium on Personal, Indoor and Mobile Radio Communications*, vol. 3, pp. 2192-2196, Sept. 2004.

[23] S. Seo, T. Dohi, and F. Adachi, "SIR-based transmit power control of reverse link for coherent DS-CDMA mobile radio," *IEICE Trans. Commun.*, vol. E81-B, no. 7, pp. 1508-1516, July 1998.

[24] J. Wen, L. Yeh, and J. Chiou, "Performance of short-term fading prediction-based power control method for DS-CDMA cellular mobile radio networks," *IEICE Trans. Commun.*, vol. E81-B, no.6, pp. 1231-1237, June 1998.

[25] S. Gunaratne, S. Nourizadeh, T. Jeans, and R. Tafazolli, "Performance of SIR-based power control for UMTS," *Proc., IEE 3G Mobile Commun. Technologies Second Intern. Conf.*, pp. 16-20, March 2001.

[26] A. Priantoro, M. Okada, and H. Yamamoto, "Comparison of SIR-based closed loop TPC in W-CDMA considering closed loop transmit diversity mode 1," *Proc., IEEE Region 10 conference TENCON 2004*, vol. B, pp. 525-528, Nov. 2004.

[27] H. Gombachika, R. Tafazolli and B. Evans, "A comparative study of predictive transmit power control schemes for S-UMTS," *Proc., IEE* 5^{th} *European Personal Mobile Communications Conference*, pp. 380-384, April 2003.

[28] J. Gallego, A. Valdovinos, M. Canales and J. de Mingo, "Analysis of closed loop power control modes in UTRA-FDD under time varying multipath channels," *Proc., IEEE Personal, Indoor and Mobile Radio Communications*, pp. 1616-1620, Sept. 2002.

[29] P. S. Kumar, R. D. Yates, and J. Holtzman, "Power control based on bit error rate (BER) measurements," *Proc., IEEE MILCOM*, vol. 2, pp. 617-620, Nov. 1995.

[30] R. M. Buehrer and R. Mahajan, "On the usefulness of outer-loop power control with successive interference cancellation," *IEEE Trans. Commun.*, vol. 51, no. 12, pp. 2091-2102, Dec. 2003.

[31] R. Yates, "A framework for uplink power control in cellular radio systems," *IEEE J. Selected Areas Commun.*, vol. 13, no. 7, pp. 1341-1347, Sept. 1995.

[32] J. Panicker and S. Kumar, "Effect of system imperfections on BER performance of a CDMA receiver with multipath diversity combining," *IEEE Trans. Veh. Techn.*, vol. 45, no. 4, pp. 622-630, Nov. 1996.